Marine Chemistry 250 (2023) 104196

Contents lists available at ScienceDirect

Marine Chemistry

journal homepage: www.elsevier.com/locate/marchem

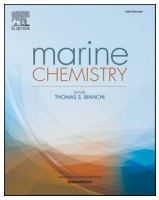

Chemical speciation models based upon the Pitzer activity coefficient equations, including the propagation of uncertainties. III. Seawater from the freezing point to 45 °C, including acid-base equilibria

Simon L. Clegg [a,*], Jason F. Waters [b], David R. Turner [c], Andrew G. Dickson [d]

[a] School of Environmental Sciences, University of East Anglia, Norwich NR4 7TJ, United Kingdom
[b] National Institute of Standards and Technology, Gaithersburg, MD 20899, USA
[c] Department of Marine Sciences, University of Gothenburg, Box 461, SE-40530 Gothenburg, Sweden
[d] University of California, San Diego, Scripps Institution of Oceanography, 9500 Gilman Drive, La Jolla, CA 92093, USA

ARTICLE INFO

Keywords:
Seawater
Pitzer model
Acid-base equilibria
Carbonate dissociation
Borate dissociation

ABSTRACT

A quantitative understanding of pH, acid-base equilibria, and chemical speciation in natural waters including seawater is needed in applications ranging from global change to environmental and water quality management. In a previous study (Humphreys et al., 2022) we implemented a model of solutions containing the ions of artificial seawater, based upon the use of the Pitzer equations for the calculation of activity coefficients and including, for the first time, the propagation of uncertainties. This was extended (Clegg et al., 2022) to include the Tris buffer solutions that are used to calibrate the seawater total pH scale. Here we apply the same methods to develop a model of solutions containing the ions of standard reference seawater, based upon studies by Millero and co-workers. We compare the predictions of the model to literature data for: the dissociation of dissolved CO_2 and bicarbonate ion; boric acid dissociation; saturation with respect to calcite, the ion product of water, and osmotic coefficients of seawater. Estimates of the uncertainty contributions of all thermodynamic equilibrium constants and Pitzer parameters to the variance of the calculated quantity are used to determine which elements of the model need improvement, with the aim of agreeing with properties noted above to within their experimental uncertainty. Further studies are recommended. Comparisons made with several datasets for carbonate system dissociation in seawater suggest which are the most reliable, and identify low salinity waters ($S < 10$) as a region for which dissociation constants of bicarbonate are not yet accurately known. At present, the model is likely to be most useful for the direct calculation of equilibria in natural waters of arbitrary composition, or for adjusting dissociation constants known for seawater media to values for natural waters in which the relative compositions of the major ions are different.

1. Introduction

Acid-base equilibria, particularly those of the carbonate system, are central to inorganic and organic speciation in natural waters generally as well as the subject of particular concern due to uptake of rising atmospheric CO_2 by the world's oceans. The total pH scale, a measure of $([H^+] + [HSO_4^-])$, has been calibrated for salinities from 20 to 40 and temperatures 0 to 40 °C (DelValls and Dickson, 1998), and stoichiometric equilibrium constants consistent with that scale (or the related seawater pH scale) have been measured for both carbonate and borate dissociation (e.g., Millero et al., 2006; Dickson, 1990). For practical use the equilibrium constants are represented by empirical equations as functions of salinity and temperature (e.g., Waters and Millero, 2013; Waters et al., 2014), and the variations of these stoichiometric constants with natural water composition are not known thus limiting their applicability to solutions of seawater stoichiometry. The same is true for the total pH scale, which is only calibrated for media of seawater composition. Furthermore, the empirical fitted equations for equilibrium constants in seawater are not subject to the constraints implied by solution theory for values at low salinities approaching freshwater conditions.

Turner et al. (2016) have elaborated the need for a chemical speciation model for seawater and related natural waters, based on the Pitzer equations (Pitzer, 1991), with potential applications in diverse areas including ocean acidification, trace metal availability, coastal and

* Corresponding author.
E-mail address: s.clegg@uea.ac.uk (S.L. Clegg).

https://doi.org/10.1016/j.marchem.2022.104196
Received 4 July 2022; Received in revised form 16 November 2022; Accepted 17 November 2022
Available online 10 December 2022

Glossary of symbols

Pitzer interaction parameters

$\beta^{(0)}_{ca}$, $\beta^{(1)}_{ca}$, $\beta^{(2)}_{ca}$, $C^{(0)}_{ca}$, $C^{(1)}_{ca}$ For interactions between cation c and anion a. Not all of these may be used, e.g., $\beta^{(2)}_{ca}$ is usually for 2:2 charge types only (e.g., $CaSO_4$), and is set to zero otherwise.

α_{ca}, $\alpha^{(2)}_{ca}$, ω_{ca} Coefficients associated with the ionic strength terms in the functions that use parameters $\beta^{(1)}_{ca}$, $\beta^{(2)}_{ca}$, and $C^{(1)}_{ca}$, respectively.

$\theta_{cc'}$, $\theta_{aa'}$ For interactions between dissimilar cations c and c', and between dissimilar anions a and a', respectively.

$\psi_{cc'a}$, $\psi_{aa'c}$ For interactions between anion a and dissimilar cations c and c', and between cation c and dissimilar anions a and a', respectively.

λ_{nc}, λ_{na} For interactions between neutral solute n and cation c, and between neutral solute n and anion a, respectively.

λ_{nn}, μ_{nnn} For the self-interaction of neutral solute n.

ζ_{nca} For interaction between neutral solute n, cation c and anion a.

Other symbols used in the text

aX Activity (molality basis) of species X, equivalent to mX·γX where γX is the activity coefficient of X.

E Electrode potential (V) in a Harned cell.

E^0 Standard electrode potential (V) of a Harned cell.

f This prefix denotes the fugacity of a gas phase species.

F The Faraday constant (96,485.33212 C mol^{-1}).

I Ionic strength, on a molality basis ($0.5\Sigma_i m_i|z_i|^2$, where z_i is the charge on ion i and the summation is over all ions).

K Thermodynamic equilibrium constant (molality basis), expressing the relationship between the quotient of the activities of the product(s) and reactant(s). It is a function of temperature and pressure. The species in parentheses is the *reactant* in an acid or base dissociation. Example: $K(HCO_3^-) = aH^+ \cdot aCO_3^{2-} / aHCO_3^-$, where a denotes activity.

K_f Thermodynamic equilibrium constant, as for K above, but for the formation of an ion pair or complex. In this case the species in parentheses is the *product* of the reaction. Examples: $K_f(MgOH^+)$, $K_f(CaCO_3^0)$.

K^* Stoichiometric equilibrium constant (on a molality basis), expressing the relationship between the quotient of the molalities of the product(s) and reactant(s). It varies with temperature, pressure, and solution composition. Example: $K^*(HCO_3^-) = mH^+ \cdot mCO_3^{2-} / mHCO_3^- = K(HCO_3^-) \cdot \gamma HCO_3^- / (\gamma H^+ \cdot \gamma CO_3^{2-})$.

mX Molality of species X (moles per kg of pure water solvent, with the units "mol kg^{-1}").

$pH^*_{T,m}$ The quantity $-\log_{10}(mH^+ + mHSO_4^-)$, where mH^+ and $mHSO_4^-$ are the conventional thermodynamic H^+ and HSO_4^- molalities. See Clegg et al. (2022) (paper II) for the relationship of this quantity to the operationally defined total pH (which is the measure in practical use), and the formal total pH.

pK $-\log_{10}$(of a thermodynamic equilibrium constant, K)

pK^* As above, but for the stoichiometric equilibrium constant K^*.

R The gas constant (8.31446 J mol^{-1} K^{-1})

T Temperature (K).

γX Activity coefficient of species X, on a molality basis.

ν_+ (or ν_c), ν_- (or ν_a) Stoichiometric numbers for the cation and anion respectively in a salt.

σ Standard uncertainty of a measured or predicted property.

ϕ Molal osmotic coefficient of a solution.

ϕ_{fp} Molal osmotic coefficient of a solution at its freezing point with respect to ice, determined from measurements of the freezing point and the thermodynamic properties of pure water and ice.

estuarine water quality, and pore water chemistry. The equations contain interaction parameters whose values are determined from thermodynamic data from single solute solutions and simple mixtures. They can be used to calculate activities, and thermal and volumetric properties, of solutions of arbitrary composition if the required parameters and thermodynamic values of equilibrium constants are known. Pitzer-based chemical speciation models have been developed for solutions containing the ions of seawater electrolyte by Millero and Roy (1997) (focusing on the dissolved carbonate system), Millero and Pierrot (1998), and by Pierrot and Millero (2017) who added trace metals. Models of acid-base equilibrium in solutions containing the ions of artificial seawater have been produced by Waters and Millero (2013), and by Clegg and Whitfield (1995) who included dissolved ammonia speciation.

A unified model of pH buffers and acid-base equilibria both in seawater and in natural waters containing the ions of seawater, but in differing stoichiometries, is desirable for the applications noted above. Recently, Humphreys et al. (2022), hereafter referred to as paper (I), have implemented an amended version of the model of Waters and Millero (2013), including for the first time the propagation of uncertainties. They validated the model against available measurements of HCl activities for acidified artificial seawater. The significance and possible applications in the field of pH are described by Clegg et al. (2022), hereafter referred to as paper (II), who extended the model of Humphreys et al. (2022) to include the Tris buffers used to calibrate the total pH scale.

In this work we implement an amended version of the Pitzer speciation model of Millero and Pierrot (1998) for solutions containing the ions of standard seawater. Some later modifications by Pierrot and Millero (2017) are included. The model incorporates the propagation of uncertainties for all calculated quantities, using the methods described in paper (I). We compare model predictions, for different salinities and temperatures, with measured values of the two carbonate dissociation constants, the dissociation constant of borate, the solubility product of solid calcite, the ion product of water, and the osmotic coefficient of seawater. Analysis of the individual uncertainty contributions of thermodynamic equilibrium constants and Pitzer interaction parameter enables us to identify elements of the model for which further work is needed in order that the model reproduce the measurements for seawater solutions to close to or within experimental uncertainty. These comparisons also yield insights into the differences between some of the datasets for dissociation of the carbonate system in seawater, including the need for improved values for the dissociation constant of bicarbonate at low salinities.

2. The speciation model

The model of artificial seawater described in papers (I) and (II) contains the principal solutes Na^+, Mg^{2+}, Ca^{2+}, K^+, Cl^-, and SO_4^{2-}. There are, in addition, the species H^+, OH^-, $MgOH^+$, and HSO_4^- that take part in acid-base equilibria. In the model of seawater presented here (based on the Reference Composition of Millero et al., 2008) there are the further species Sr^{2+}, Br^-, F^- and HF, carbonate (as CO_2*, HCO_3^-, and CO_3^{2-}), and borate ($B(OH)_4^-$ and $B(OH)_3$). The species CO_2* is the

combined amounts of $CO_{2(aq)}$ and $H_2CO_{3(aq)}$, which are not distinguished. The former is by far the dominant species (Soli and Byrne, 2002). The following ion pairs and minor species were also found to be necessary by Millero and Pierrot (1998) and are included in the model: MgF^+, CaF^+, $MgCO_3^0$, $CaCO_3^0$, and $SrCO_3^0$. There are a total of 12 equilibria in this system, which are summarised in Table 1. In the table we also list the symbols used for the various thermodynamic equilibrium constants and, for convenience, those for the corresponding stoichiometric constants defined in the second chapter of Dickson et al. (2007). We have not yet included in the model other minor components from the work of Millero and Pierrot (1998) or Pierrot and Millero (2017).

The major species noted above, and therefore many of the Pitzer model interactions, are common to the models of Waters and Millero (2013) and of Millero and Pierrot (1998). However, a number of the parameter values (for the same interactions) differ, which can be attributed partly to the fact that there are fifteen years separating the two publications. In this work we have not attempted to make the two models consistent, i.e., use the same sets of parameter values for the species they have in common, although this is desirable as a long-term goal. The differences are described in Section 2.2.

The Pitzer expressions for the activity coefficients (γ) of ions and uncharged species are described by Pitzer (1991, and references therein), and in the Appendix to Clegg et al. (1994) for ion-ion interactions, and are not reproduced here. They include parameters, which vary with temperature and pressure, for the interactions of pairs and triplets of solute species. The parameters for ion interactions are: $\beta^{(0)}_{ca}$, $\beta^{(1)}_{ca}$, $\beta^{(2)}_{ca}$, $C^{(0)}_{ca}$, and $C^{(1)}_{ca}$ for combinations of each cation c and each anion a; $\theta_{cc'}$ and $\psi_{cc'a}$ for each pair of dissimilar cations c and c', and anion a; and $\theta_{aa'}$ and $\psi_{aa'c}$ for each pair of dissimilar anions a and a', and cation c. The parameters for the interaction of ions and neutral solutes (such as CO_2* and $B(OH)_3$, or ion pairs such as $MgCO_3^0$) are $\lambda_{n,i}$ and $\zeta_{n,c,a}$, where n is the neutral species, and i is any cation or anion. These parameters are listed in the Glossary of Symbols, together with definitions of other symbols used in this work.

It should be noted that parameters $\lambda_{n,c}$ and $\lambda_{n,a}$ can only be determined as combinations $[(\nu_+)\lambda_{n,c} + (\nu_-)\lambda_{n,a}]$, where ν_+ and ν_- are the stoichiometric numbers of cation c and anion a in an electrolyte. Because of this, it is conventional to set the $\lambda_{n,i}$ parameter to zero for one ion i for each electrolyte. In this model of seawater, $\lambda_{n,i}$ are set to zero for the interaction of H^+ with CO_2* and $B(OH)_3$, and for Cl^- with HF and $MgCO_3^0$ (parameters $\lambda_{n,i}$ for $CaCO_3^0$ and $SrCO_3^0$ are unknown). The choice of interactions to set to zero in this way does not affect the calculation of the mean activity coefficients of pairs of ions, or chemical speciation (i.e., concentrations at equilibrium), but *does* change formal calculated single ion activities.

The model is solved, to obtain the equilibrium speciation and solute and solvent activities, using the same Gibbs energy minimisation approach used by Humphreys et al. (2022) (see the Supporting Information to that paper) and, earlier, by Wexler and Clegg (2002). Further information, for the additional species in the present model, are provided in the Supporting Information to this work.

2.1. Changes to the model

The primary source of parameters and equilibrium constants is Millero and Pierrot (1998), and references cited therein. We have checked values against those in the original cited articles, and have identified a number of corrections. These are documented in the Supporting Information. There are also some ambiguities in citations, and interaction parameters whose values we were not able to reconcile with

Table 1
Equilibrium reactions in the model of standard seawater, and the assumed uncertainties of the equilibrium constants at 25 °C.

Thermodynamic equilibrium constant	Type [a]	Reaction [b]	Std. uncert. (σ) in ln(K)	Corresponding stoichiometric quantity [c]	Note
$K(HSO_4^-)$	d	$HSO_4^- \leftrightarrow H^+ + SO_4^{2-}$	0.048	K_S	[d]
$K(CO_2^*)$	d	$CO_2^* + H_2O \leftrightarrow HCO_3^- + H^+$	0.005	K_1	[e]
$K(HCO_3^-)$	d	$HCO_3^- \leftrightarrow CO_3^{2-} + H^+$	0.007	K_2	[f]
$K(B(OH)_4^-)$	d	$H^+ + B(OH)_4^- \leftrightarrow B(OH)_3 + H_2O$	0.0046	$1/K_B$	[g]
K(HF)	d	$HF \leftrightarrow H^+ + F^-$	0.015	K_F	[j]
$K(H_2O)$	d	$H_2O \leftrightarrow H^+ + OH^-$	0.023	K_W	[h]
$K_f(MgOH^+)$	f	$Mg^{2+} + OH^- \leftrightarrow MgOH^+$	0.022	–	[i]
$K_f(MgF^+)$	f	$Mg^{2+} + F^- \leftrightarrow MgF^+$	0.0576	–	[k]
$K_f(CaF^+)$	f	$Ca^{2+} + F^- \leftrightarrow CaF^+$	0.0576	–	[l]
$K_f(MgCO_3^0)$	f	$Mg^{2+} + CO_3^{2-} \leftrightarrow MgCO_3^0$	0.055	–	[m]
$K_f(CaCO_3^0)$	f	$Ca^{2+} + CO_3^{2-} \leftrightarrow CaCO_3^0$	0.055	–	[n]
$K_f(SrCO_3^0)$	f	$Sr^{2+} + CO_3^{2-} \leftrightarrow SrCO_3^0$	0.055	–	[n]

Notes: Equations for the equilibrium constants as functions of temperature are presented in the Supporting Information.

[a] Indicates whether the reaction is formation 'f' of the indicated species, or dissociation 'd' of the species.

[b] The reaction to which the equilibrium constant applies.

[c] This column lists the symbols used for the stoichiometric equilibrium constants in the *Guide to Best Practices for Ocean CO_2 Measurements* (Dickson et al., 2007). Note that these are defined on an amount content (moles per kg of seawater) basis rather than molality.

[d] The value of σ is the 25 °C value given in Table II of Dickson et al. (1990) (converted to a natural logarithm).

[e] The assigned value of σ is that for an approximate 2σ precision of fit to the data for "freshwater values" for the dissociation of CO_2* to HCO_3^- (K_1), see Section 7 of Lewis and Wallace (1998). We contrast these values with standard deviations equivalent to 0.003 in ln($K(CO_2^*)$) obtained by Harned and Davis (1943), and 0.0037 in ln($K(HCO_3^-)$) by Harned and Scholes (1941). In both cases these standard deviations are of measured values about their fitted equations (functions of temperature).

[f] The value of σ is that for the 2σ precision of a fit to the data, for a freshwater value of the equilibrium constant (Lewis and Wallace, 1998). See also note (e) above.

[g] The source of σ is the observation of Owen (1934), referring to the pK_a of boric acid, that: "The internal consistency of the various series points to an accuracy of about ±0.002 in pK" (hence ±0.0046 in ln(K)).

[h] The value of σ (equivalent to ±0.01 in $\log_{10}(K)$) is that given by Marshall and Franck (1981) for their expression for the ion product of water which was used in the model of Clegg and Whitfield (1995). It is assumed to apply to the simpler expression used by Millero and Pierrot (1998), based upon the work of Harned and Owen (1958), for the present model.

[i] The uncertainty in ln($K_f(MgOH^+)$) is essentially unknown. The value σ used both in this work and in paper (I) is based upon the fact that Harvie et al. (1984) assigned a pK_d of 2.19, which implies an uncertainty of at least 0.0115 in ln($K_f(MgOH^+)$). We approximately doubled this value to an assumed σ equal to 0.022.

[j] The source of σ is the uncertainty given for 15 °C by Broene and De Vries (1947).

[k] The value of σ was estimated as follows: the average of the standard deviations listed in Table 1 of Elgquist (1970) is 1.2 in K_f*(MgF^+) (on a molarity basis) for ionic strengths 0.1 to 1.0 mol dm^{-3}. Applying this average to the thermodynamic value at 25 °C yields an uncertainty of about 0.025 in $\log_{10}(K)$, hence 0.0576 in ln(K).

[l] Assumed to be the same as for ln($K_f(MgF^+)$) above.

[m] The value of σ is from Millero and Thurmond (1983) (0.024 in $\log_{10}(K^*)$, over a range of ionic strengths).

[n] Assumed to have the same uncertainty as ln($K_f(MgCO_3^0)$).

those in the source articles. In these cases it was necessary to make assumptions, or to refit the data. The more important of the changes we have made are summarised below.

First, the parameters for interactions between Na^+ and HSO_4^- in the model were obtained from measured EMFs of HCl-Na_2SO_4 solutions over a range of temperatures (Pierrot et al., 1997). We redetermined their values in this study in order to be consistent with the revised values of $\theta_{H,Na}$ and $\psi_{H,Na,Cl}$ obtained in paper (I) (the same values of these parameters were used in the models of both Millero and Pierrot (1998) and Waters and Millero (2013)).

Second, Millero and Pierrot (1998) list temperature dependent $\beta^{(0)}_{Ca,SO4}$ and $\beta^{(1)}_{Ca,SO4}$ parameters from Møller (1988) in their table A1. However, the model of Millero and Pierrot does not include the ion pair $CaSO_4^0$ used by Møller (1988), and the use of values of $\beta^{(0)}_{Ca,SO4}$ and $\beta^{(1)}_{Ca,SO4}$ alone to quantify Ca^{2+}-SO_4^{2-} interactions would therefore not yield correct results. For this reason, we have adopted interaction parameters from paper (I), which include a $\beta^{(2)}_{Ca,SO4}$ term to account for the effects of ion association (e.g., Pitzer, 1991). Interactions between Sr^{2+} and SO_4^{2-} are treated identically to those for Ca^{2+} and SO_4^{2-} (i.e., their interaction parameters are assumed to be the same).

Third, we have followed the recommendation of Hain et al. (2018), and adopted values of $\beta^{(0)}_{Ca,HCO3}$ and $\beta^{(1)}_{Ca,HCO3}$ from the study of He and Morse (1993).

Fourth, Millero and Pierrot (1998) cite Millero and Thurmond (1983) for the relationship $\log_{10}(\gamma MgCO_3^0)$ equal to $0.0560{\cdot}I$ (where I is the molality-based ionic strength) at 25 °C in aqueous NaCl containing small additions of $MgCl_2$. We obtained a value of $\lambda_{MgCO3,Na}$ equal to 0.0745 from the Pitzer equation for the activity coefficient of a neutral solute (e.g., eq. (75) of Pitzer (1991)) by attributing all of the ionic strength of the solutions to NaCl (hence I equal to $1.156{\cdot}m$NaCl), and setting $\lambda_{MgCO3,Cl}$ equal to zero.

Values and equations for all model parameters are presented in the Supporting Information to this work.

2.2. Differences from the model of artificial seawater

The model of seawater electrolyte described in this work differs in some respects from that described in papers (I) and (II) for artificial seawater. The model of artificial seawater includes the solute species H^+, Na^+, Mg^{2+}, Ca^{2+}, K^+, $MgOH^+$, Cl^-, SO_4^{2-}, HSO_4^- and OH^-; and equilibria for $MgOH^+$ formation, and HSO_4^- and water dissociation. The model in paper (II) adds the buffer species $TrisH^+$ and Tris, and the equilibrium between them, but is otherwise the same. The present model contains the same equilibria as in paper (I), and the same expressions for the equilibrium constants as functions of temperature. The cation-anion interaction parameters in the models that differ are those for: Na^+-SO_4^{2-}, Na^+-HSO_4^-, Mg^{2+}-HSO_4^-, Mg^{2+}-Cl^-, Ca^{2+}-HSO_4^-, K^+-SO_4^{2-}, and K^+-OH^-. There are other differences for the ternary cation-cation-anion and anion-anion-cation interactions that are not listed here (the values, and all sources, are listed in the Supporting Information to this work and to paper (I)). It is desirable that both models eventually converge on the same set of interaction parameters, and equilibrium constants, for the common constituent species on grounds of simplicity and for self-consistency. The latter may be particularly important because solutions of Tris buffer in artificial seawater are used to calibrate the total pH scale used by marine scientists, which is the basis of the stoichiometric equilibrium constants that have been determined for the carbonate and borate systems in seawater. We envisage further development of both the model of Tris buffer in artificial seawater and that for seawater electrolyte, and some of the required improvements – for example in the representation of HSO_4^-/SO_4^{2-} equilibrium – are the same for both models. The eventual use of a common set of parameters and equilibrium constants, for the ions present in artificial seawater, will make future extensions to include other species simpler and ensure consistency between model calculations for seawater solutions and for Tris pH buffer in artificial seawater.

3. Treatment of uncertainties

Estimated variances of model-predicted pH, activities, and other properties are calculated by standard methods of error propagation such as used by Orr et al. (2018). Their application to the speciation model used here is described in detail in paper (I). As is the case for the model of Waters and Millero (2013) for artificial seawater, variances and covariances of the Pitzer interaction parameters are not available, and we have adopted the same simplified method of estimating them. This is based upon the assumption that all parameters were obtained by fitting to single datasets of osmotic coefficients (ϕ), which were assumed to be subject to the random and systematic errors that are typical of isopiestic measurements of water activity. This measurement is one of the main methods of activity determination for solutions of non-volatile electrolytes at room temperature and above (Rard and Platford, 1991). Parameter variances and covariances were determined from the statistics of multiple fits of artificial datasets of osmotic coefficients generated by the model and then perturbed by randomly generated errors both for individual points (random error) and affecting the entire artificial dataset (systematic error).

In the model of artificial seawater in paper (I) there are only ten solute species and two chemical equilibria. The addition of Tris buffer substances to that model (paper (II)) adds two further species, and one equilibrium. In the present model of seawater electrolyte there are nine cations, nine anions, six uncharged solute species, and thirteen equilibria. This is a greatly more complex system, and there are potentially a very large number of binary and ternary Pitzer ion-ion and ion-neutral interaction parameters – more than an order of magnitude more than for the other two models. There are many potentially significant interaction parameters whose values are unknown (and therefore set to zero), and it is important both to be able to assess their possible contribution to the uncertainties of model-calculated quantities and, particularly, to determine which of the unknown interactions might account for deviations between measured and model-calculated properties and therefore require further study. In the next section we characterise the unknown ion-ion and ion-neutral interactions, in order to determine which of these should be included in the treatment of uncertainties. In Section 3.2 we briefly describe the procedure for simulating parameter variances, including some additions to that used in papers (I) and (II) in order to include some key ion-neutral interactions.

3.1. Pitzer interaction parameters whose values are unknown

It is necessary, first, to reduce the very large set of unknown possible ion-ion and ion-neutral interactions to a smaller group consisting only of those which are likely to have a significant influence on calculated properties of natural waters of broadly seawater composition, and which are likely to be determinable from measurements. All unknown interactions were therefore characterized according to a simple set of criteria based upon their relative molality (fraction of the total molality) in standard seawater, their participation in chemical reactions (which usually renders interaction parameters for the reactants and product redundant), and whether the interaction parameters were explicitly set to zero in the application of the model to a particular subset of species. These categories are defined in Section 1, and in Tables S2 to S6, of the second document of the Supporting Information. The unknown interactions that are possibly significant in the model of seawater electrolyte are identified in the tables. These include three cation-anion interactions, sixteen $\theta_{cc'}$ and $\psi_{cc'a}$, fifteen $\theta_{aa'}$ and $\psi_{aa'c}$, three λ_{nc}, and three λ_{na}. Many of these parameters are only significant if properties of the solute species involved (e.g., Br^-, F^-) are of interest. This is because minor and trace species such as these are at very low concentration in seawater and do not significantly affect the principal acid-base equilibria, although we note that HF is included in the definition of pH on the seawater scale. Unknown values of parameter ζ_{nca} have been ignored in this assessment, because they do not have a significant influence at

seawater molalities.

We identified three ways of addressing the possible influence of unknown parameters on calculated speciation and on the uncertainties of model-calculated quantities.

(i) Set the unknown parameters to zero (the usual approach), and their variances and covariances to zero so that they neither influence the calculated equilibrium speciation in the solution nor the estimated uncertainties of any calculated properties. This is the simplest possible approach, and is reasonable given that values of some of the interaction parameters in the model were derived on the assumption that others are equal to zero. An example is the mixture H^+-Na^+-SO_4^{2-}-HSO_4^--H_2O: in the work of Harvie et al. (1984) the ternary parameters $\psi_{H,Na,SO4}$, $\psi_{HSO4,SO4,H}$ and $\theta_{HSO4,SO4}$ are all zero. The latter two parameters are zero because they were also set to this value in the model treatment of aqueous H_2SO_4, and $\psi_{H,Na,SO4}$ because it was found to be unnecessary or redundant.

(ii) Set the unknown parameters to zero in the same way as for (i), but assume that they have been determined in the same way as other (non-zero) parameters. Thus their uncertainties are simulated in the same way, and are found to have variances and covariances that are comparable. In this approach calculated equilibrium speciation and activities are the same as for the previous case – because the values of the unknown parameters are still zero – but the estimated uncertainties of calculated quantities are increased to some degree. Examples of unknown, but potentially significant, interaction parameters are $\theta_{Na,MgOH}$, $\lambda_{CaCO3,Na}$, and $\lambda_{B(OH)3,Mg}$. These are all interactions of major seawater ions with minor species that are significant in the estimation of several properties (the ion product of water, carbonate acid-base equilibrium and calcite saturation, and borate acid-base equilibrium, respectively).

(iii) Set the unknown parameters to averaged values determined from published results for the same interaction parameters but for many different species, and assign variances equal to the squares of the standard deviations of the averaged values. Such variances are very much larger than those for category (ii) above, but may be more representative of the influence of unknown, but probably non-zero, parameters on the uncertainty of model-calculated speciation. Because of the use of average parameter values (rather than zero), the calculated speciation will differ from the base case. Averaged values, and their standard deviations, are listed in Appendix A of paper (I) for different parameter types. We note that the averaged values for most ternary interaction parameters (table A2 of paper (I)) differ from zero by less than one standard deviation, so an alternative approach would have been to retain zero as the values of the unknown parameters, but use the larger uncertainty (i.e., the standard deviation associated with that average). The behaviour of $\beta_{ca}^{(0)}$ and $\beta_{ca}^{(1)}$ parameters for cation-anion interactions is more complex: values of the two parameters are correlated, and we have taken this into account in their treatment (table A1 of paper (I)).

In the majority of calculations presented in this work we have taken approach (i) above, for simplicity and to easily assess the performance of the base model. The second and third approaches are necessary to determine the significance of unknown interaction parameters for various calculated quantities, and where they have been used it is stated explicitly.

3.2. Simulations to obtain estimated variances and covariances of interaction parameters

The method for estimation of variances and covariances used here is the same as described in Section 3.2 of paper (I). It corresponds to how Pitzer-based chemical speciation models of mixtures are typically developed, and is briefly summarised in this section. We also describe some additional procedures that were used for the principal neutral-ion interaction parameters. Variances and covariances of ion-ion binary and ternary interaction parameters were obtained as follows: first, for cation-anion interactions and up to five of the parameters $\beta_{ca}^{(0-2)}$, and $C_{ca}^{(0,1)}$; second, for parameters $\theta_{cc'}$ and $\psi_{cc',Cl}$ from simulations of ternary chloride solutions (e.g, aqueous Na^+-Mg^{2+}-Cl^-); third, for parameters $\theta_{aa'}$ and $\psi_{aa',Na}$ from simulations of ternary solutions containing Na^+ and two dissimilar anions (e.g, aqueous Na^+-Cl^--SO_4^{2-}). Next, variances of $\theta_{cc'}$ obtained previously were used in simulations of ternary solutions containing the same cations c and c', and anion a (where $a \neq Cl^-$), to obtain a variance for $\psi_{cc'a}$ and its covariance with $\theta_{cc'}$. Similarly, variances of parameters $\theta_{aa'}$ were used in simulations to obtain variances of $\psi_{aa'c}$ (where cation $c \neq Na^+$), and its covariance with $\theta_{aa'}$. Details of the methods and programs used are given in the Supporting Information to paper (I).

In the present model there are six uncharged species, and the most important ones for acid-base equilibrium are CO_2* (which is not distinguished from the very small fraction present as H_2CO_3) and $B(OH)_3$. For both species n some ζ_{nca} parameters are known, in addition to λ_{nc} and λ_{na}. For these species we have obtained estimates of the variances of non-zero values of ζ_{nca} only, in addition to variances of parameters λ_{nc} and λ_{na} for interactions with ions Na^+, Mg^{2+}, Ca^{2+}, K^+, Cl^- and SO_4^{2-}. For CO_2* and $B(OH)_3$ the reference ion for the interactions is H^+ (thus $\lambda_{CO2,H}$ and $\lambda_{B(OH)3,H}$ are defined to be zero), whereas for the other neutral solutes it is Cl^- (hence $\lambda_{n,Cl}$ is equal to zero in these cases).

We first assumed that variances and covariances of interaction parameters for CO_2* and $B(OH)_3$ could be obtained from simulations that corresponded to the fitting of parameter values in the following order:

(i) Values for $\lambda_{n,Cl}$ and $\zeta_{n,H,Cl}$ (n is CO_2* or $B(OH)_3$) from simulations for CO_2* -HCl and $B(OH)_3$-HCl solutions.

(ii) Values for $\lambda_{n,SO4}$ only from simulations for CO_2* -H^+-SO_4^{2-} and $B(OH)_3$-H^+-SO_4^{2-} solutions. These simulations were simplified in that HSO_4^- formation was ignored, and the only ions present were therefore H^+ and SO_4^{2-}.

(iii) Values for $\lambda_{n,M}$ and $\zeta_{n,M,Cl}$ from data for solutions containing CO_2* or $B(OH)_3$ and the chloride salts of the major seawater cations M (Na^+, Mg^{2+}, Ca^{2+}, and K^+). The variance of $\lambda_{n,Cl}$ is already known, which enables covariances with $\lambda_{n,M}$ and $\zeta_{n,M,Cl}$ to be obtained.

(iv) Variances of $\zeta_{n,M,SO4}$, and covariances between $\lambda_{n,SO4}$ and $\lambda_{n,M}$, and between these two binary parameters and $\zeta_{n,M,SO4}$, from data for solutions containing CO_2* or $B(OH)_3$ and the sulphate salts of cations M (Na^+, Mg^{2+}, and K^+).

In this way it is possible to obtain estimates of the variances and covariances of the groups of parameters [$\lambda_{n,M}$, $\lambda_{n,Cl}$, and $\zeta_{n,M,Cl}$], and [$\lambda_{n,M}$, $\lambda_{n,SO4}$, and $\zeta_{n,M,SO4}$]. However, this procedure fails to capture a large positive covariance between parameters $\lambda_{n,c}$ and $\lambda_{n,c'}$ (where c and c' are two seawater cations) resulting in overall uncertainty contributions being too low. We therefore chose to simplify the treatment of these groups of parameters by re-deriving the variances setting covariances cov($\lambda_{n,M}$, $\lambda_{n,Cl}$) and cov($\lambda_{n,Cl}$, $\zeta_{n,M,Cl}$) to zero for all seawater cations M. We left the variances and covariances involving the corresponding SO_4^{2-} parameters unchanged (their contributions to total uncertainties are much less, given that the ratio of Cl^-:SO_4^{2-} in seawater is 1:0.052). This is reasonable given the other assumptions and approximations inherent in the estimation of uncertainties for these ternary parameters. Further information concerning the determination of variances for neutral-ion interaction parameters, and the positive covariance noted above, can be found in the third document of the Supporting Information.

For other neutral species (for which only a few ion interactions have been quantified) we have simulated variances of λ_{nc} and λ_{na} only, for a

smaller set of major seawater ions in accordance with the classification scheme for unknown parameters described earlier. Variances of parameters $\lambda_{n,M}$, where M is a seawater cation, were obtained from simulations of mixtures containing chloride salts of the metal cations. Variances of parameters $\lambda_{n,SO4}$ and $\lambda_{n,HCO3}$ were obtained from simulations of mixtures containing Na_2SO_4 and $NaHCO_3$, respectively. For simplicity, no covariances were estimated.

Values of all variances and covariances are listed in the fourth and fifth documents of the Supporting Information.

3.3. Equilibrium constants

The estimated uncertainties (σ) of the logarithms of these quantities, at 25 °C, are listed in Table 1 together with brief explanations of how these were assigned. The uncertainties are themselves poorly quantified, and in several cases assumptions have had to be made.

4. Acid-base equilibria in seawater electrolyte

The conventional thermodynamic total pH (which is also the value calculated using the speciation model), $pH^*_{T,m}$, is given by:

$$pH^*_{T,m} = -\log_{10}(mH^+ + mHSO_4^-) \quad (1)$$

where prefix (and subscript) m denotes molality, and quantity mH^+ is the free hydrogen ion molality. A similar expression can be written for pH on the seawater scale, $pH^*_{SWS,m}$, which includes the associated species HF:

$$pH^*_{SWS,m} = -\log_{10}(mH^+ + mHSO_4^- + mHF) \quad (2)$$

The superscript * is used to indicate that both measures of pH are conventional thermodynamic values. This measure of total pH (Eq. (1)) should be distinguished from the pH_T established by DelValls and Dickson (1998). They differ because of assumptions made in both the definition of the total pH scale and its calibration using Tris buffers, and are related to the fact that mean activity coefficients of HCl and values of the stoichiometric dissociation constant of HSO_4^-, $K^*(HSO_4^-)$, in the artificial solutions containing finite amounts of Tris and $TrisH^+$ are not the same as in pure artificial seawater of the same nominal salinity and temperature. The difference between $pH^*_{T,m}$ and pH_T (when also expressed on a molality basis) has been quantified, for the first time, by Clegg et al. (2022) and is found to be 0.0045 ± 0.0014 in pH_T for a 0.04 mol kg^{-1} Tris buffer at salinity 35 and 25 °C. This is small compared to the uncertainties in the experimental values of the stoichiometric dissociation constants of the carbonate system in seawater, and is not considered further here. In the model calculations in this work only the conventional thermodynamic free and total H^+ molalities are used.

In addition to acid-base equilibria involving carbonate species, borate, sulphate, and fluoride there are a number of ion pairing reactions: F^- with Mg^{2+} and Ca^{2+}, OH^- with Mg^{2+}, and particularly CO_3^{2-} with Mg^{2+}, Ca^{2+} and Sr^{2+}. The latter influence the modelled pH of seawater electrolyte, and also the degree of saturation with respect to calcite. In a seawater similar to the Reference Composition (table 4 of Millero et al., 2008), $pH^*_{T,m}$ equal to 8.1, and 25 °C, we obtain the following speciation: HSO_4^- and HF are 28% and 2.8% of the free H^+ molality, respectively; CO_2^*, HCO_3^-, and CO_3^{2-} are 0.48%, 87.7% and 5.06% of the total dissolved inorganic carbon, respectively, and $MgCO_3^0$, $CaCO_3^0$, and $SrCO_3^0$ ion pairs together are 6.75%; and $B(OH)_3$ is 76% of total boron (the remainder is $B(OH)_4^-$). Small amounts of fluoride are also present as MgF^+ (about one third of total F^-) and CaF^+.

A satisfactory model of pH, carbonate speciation, and calcium carbonate saturation in seawater needs to model most of the above equilibria accurately. The data we use to evaluate the model have been chosen with this in mind, although we note that there are no direct measures of ion pairing equilibria.

5. Data used to assess the model

We compare the model to measurements of osmotic coefficients and various stoichiometric dissociation constants in seawater and artificial seawater in order to assess its performance for the calculation of key acid-base equilibria and also the degree of calcite saturation. Osmotic coefficients are chiefly a test of the ability of the model to calculate the interactions of major ions (Na^+, Mg^{2+}, Cl^- and SO_4^{2-}) and their effect on water activity, which is also relevant to the prediction of the ion product of water. The data sources are listed in Table 2, and include the principal studies of dissolved carbonate speciation (seven sources), and single sets of measurements of the ion product of water ($K^*(H_2O)$), borate dissociation ($K^*(B(OH)_4^-)$), and calcite saturation ($K^*(CaCO_{3(s)})$). We did not include the EMF data for borate dissociation in seawater of Roy et al. (1993a) because they state that their measurements are in excellent agreement with those of Dickson (1990).

Table 2
Sources of data with which the model is compared.

Quantity[a]	pH[b]	t (°C)	Salinity[c]	Medium[d]	F^-[e]	Study	Note
ϕ	–	25	17.054–37.96	seawater/ASW	yes	Robinson (1954)	
ϕ_{fp}	–	−0.208 to −2.220	3.78–40.20	seawater	yes	Doherty and Kester (1974)	
ϕ_{fp}	–	−0.954 to −1.921	17.74–35.00	seawater	yes	Fujino et al. (1974)	
$K^*(H_2O)$	–	5–35	10.43–47.78	ASW	yes	Dickson and Riley (1979)	
$K^*(B(OH)_4^-)$, EMF	total	0–45	5.01–45	ASW	no	Dickson (1990)	
$K^*(CO_2^*)$, $K^*(HCO_3^-)$	total	0–45	5–45	ASW	no	Roy et al. (1993b)	[f]
$K^*(CO_2^*)$, $K^*(HCO_3^-)$	SWS	−1.21–40.67	9.858–49.731	ASW	yes	Goyet and Poisson (1989)	
$K^*(CO_2^*)$, $K^*(HCO_3^-)$	total	2–35	19.16–42.94	seawater	yes	Lueker et al. (2000)	
$K^*(CO_2^*) \times K^*(HCO_3^-)$	SWS	9.948–44.976, 4.923–44.976	14.993–39.96, 5.023–41.838	seawater	yes	Prieto and Millero (2002)	
$K^*(CO_2^*)$	SWS	14.9–24.99	10.08–39.96	seawater	yes	Prieto and Millero (2002)	
$K^*(CO_2^*)$, $K^*(HCO_3^-)$	SWS	1.0–50.4	0.953–50.754	seawater	yes	Millero et al. (2006)	
$K^*(CO_2^*) \times K^*(HCO_3^-)$	total	15.05–35.02	19.62–40.98	seawater	yes	Schockman and Byrne (2021)	[g]
$K^*(CaCO_{3(s)})$	–	5–40	5–44	seawater	yes	Mucci (1983)	

Notes:
[a] Measured osmotic coefficients (ϕ, and ϕ_{fp}), and stoichiometric equilibrium constants as indicated.
[b] The pH scales are total and seawater (SWS).
[c] The listed salinities are practical salinities (seawater media), and nominal practical salinities (ASW). The seawater samples in the measurements of Robinson (1954) were both natural and artificial. They were converted to salinity by multiplying the listed chlorinities by the factor 1.80655 (Millero et al., 2008).
[d] Seawater – natural seawater; ASW – artificial seawater.
[e] Indicates whether the medium contains fluoride or not.
[f] Including errata for both $\ln(K^*)$ determined from the measured EMFs (Roy et al., 1994), and the fitted equation for $\ln(K^*(CO_2^*))$ (Roy et al., 1996).
[g] These results, which were obtained spectrophotometrically, were adjusted so that they are based upon $pK_2^T e_2$ of either Douglas and Byrne (2017) (for salinity 19.62) or Liu et al. (2011) (the rest).

All salinities listed in the tables in this work, and used in figures, are practical salinities (or nominal practical salinities in the case of artificial seawaters) unless otherwise stated. When comparing with quantities measured in natural seawater we have used the composition listed by Millero et al. (2008) in their table 4.

6. Assessment of the model

Here the predictions of the model are compared with measured stoichiometric equilibrium constants, EMFs, and other data from sources in Table 1. We have also determined mean deviations and standard deviations for pK^*, for the first and second acid dissociation constants of carbon dioxide, $K^*(CO_2^*)$ and $K^*(HCO_3^-)$, with respect to both model predictions and the empirical fitted equation of Millero (2010) as corrected by Waters and Millero, 2013; Waters et al., 2014). We have done the same for the dissociation of borate (both data and empirical fitted equation taken from Dickson, 1990).

The inclusion of many studies of dissolved carbonate equilibria allows the measurements to be compared to each other, as well as to the model, and for both data and empirical fitted equations to be assessed to determine whether their behaviour is realistic at low salinities and in the approach to infinite dilution (pure water). We have combined the presentation of these comparisons, below, with the results of calculations of the uncertainty contributions of individual Pitzer parameters and thermodynamic equilibrium constants to model-calculated properties in order to determine which elements of the model are most likely to account for observed deviations between the model and data.

6.1. Total pH and the stoichiometric carbonate dissociation constants

We first consider the relative uncertainty contributions of the Pitzer model parameters, and thermodynamic equilibrium constants, to the estimated total variance of model-calculated $pH^*_{T,m}$, $\ln(K^*(CO_2^*))$, $\ln(K^*(HCO_3^-))$, and $\ln(K^*(CO_2^*)\cdot K^*(HCO_3^-))$. These contributions are shown in Fig. 1, for salinity 35 seawater electrolyte and 25 °C, and can be considered as an indicator of those model elements most likely to account for errors (differences between model predictions and measurements). Only the top fifteen values are shown, in each case, because

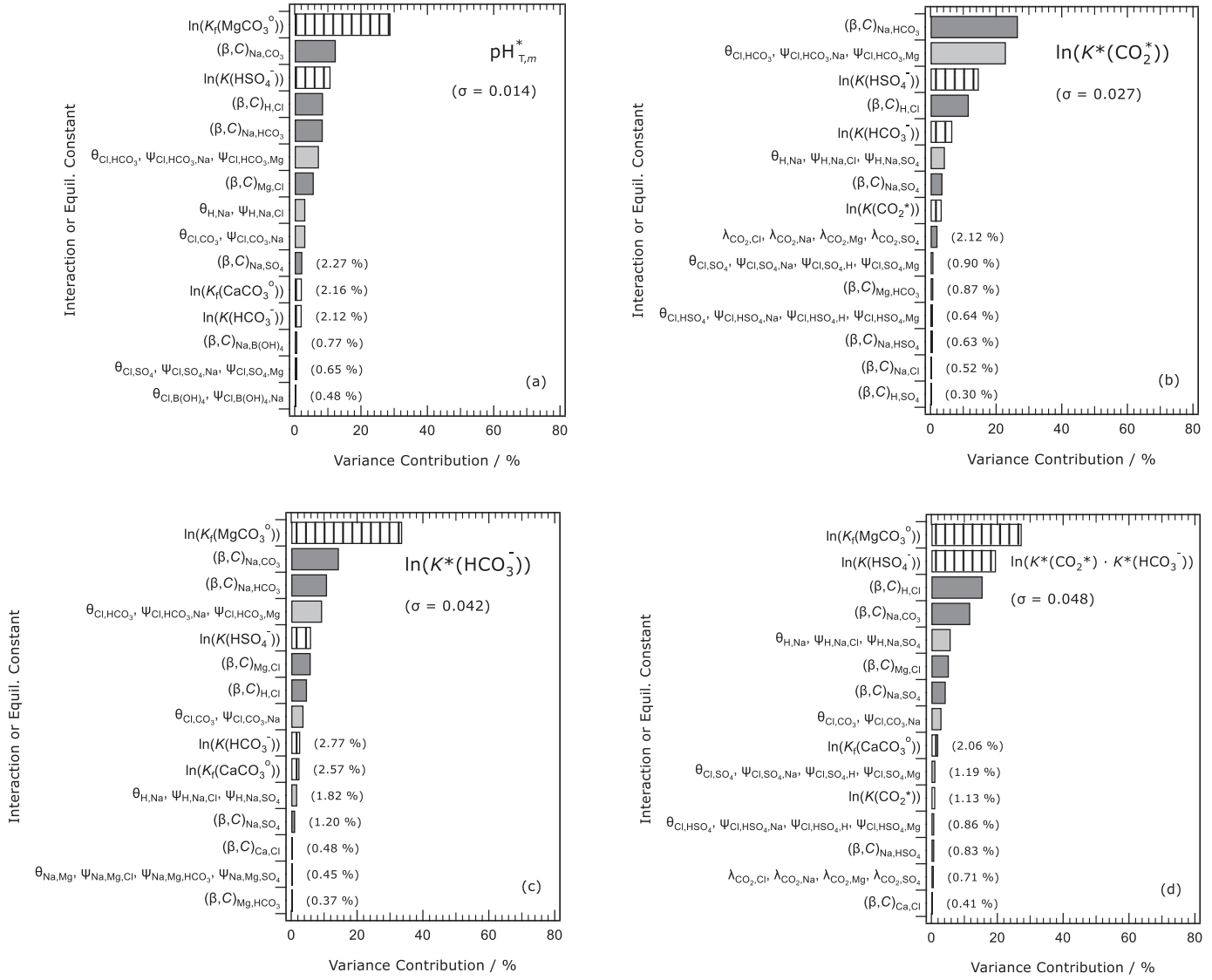

Fig. 1. Percentage contributions of individual Pitzer model interactions, and equilibrium constants, to the variances of several model-calculated quantities in salinity 35 seawater at 25 °C. (a) $pH^*_{T,m}$, total pH ($-\log_{10}(mH^+ + mHSO_4^-)$); (b) $\ln(K^*(CO_2^*))$, the log of the stoichiometric dissociation constant of CO_2; (c) $\ln(K^*(HCO_3^-))$, the log of the stoichiometric dissociation constant of HCO_3^-; (d) $\ln(K^*(CO_2^*)\cdot K^*(HCO_3^-))$ the log of the product of the two dissociation constants. The parameters associated with each of the interactions are listed down the left-hand sides, and contributions of about 2% and below are noted on the plots. Symbols *K*(*species*) and K_f(*species*) denote the thermodynamic equilibrium constants of the named solute species, as defined in Table 1. Only the fifteen largest contributions are shown. The estimated combined standard uncertainty of the calculated quantity is given on each plot.

these account for almost all of the calculated total variance. More than 50% of the total estimated variance of $pH^*_{T,m}$, see Fig. 1a, is accounted for by uncertainties in: (i) the thermodynamic equilibrium constant $K_f(MgCO_3^0)$ (formation of the magnesium carbonate ion pair); (ii) the Pitzer parameters for Na^+-CO_3^{2-} interactions, and (iii) the thermodynamic equilibrium constant $K(HSO_4^-)$. The next most important contributions are those of the Pitzer parameters for the interactions of the major ions Cl^- and Na^+ with H^+ and HCO_3^-, respectively, and a set of mixture parameters that includes $\theta_{Cl,HCO3}$. The constant $K_f(MgCO_3^0)$ is also a major contributor to the uncertainty of $\ln(K^*(HCO_3^-))$, and is discussed further in Section 6.1.2.

The inclusion of averaged parameter values (see Section 3.1) from Appendix A of paper (I), in place of those that are unknown and normally set to zero, increased the standard deviation of the modelled $pH^*_{T,m}$ only slightly. The most important of the unknown interactions appear to be those between $B(OH)_4^-$ and Mg^{2+} (a 2.5% variance contribution), and between ion pair $CaCO_3^0$ and Na^+ (2% variance contribution).

The largest uncertainty contributions to the model calculated $\ln(K^*(CO_2^*))$, in Fig. 1b, are: the Na^+-HCO_3^- interaction, which influences the degree of CO_2^* dissociation through the activity coefficient of HCO_3^-; ternary interactions involving Cl^- and HCO_3^-; and the dissociation constant $K(HSO_4^-)$. This dissociation constant is present because the modelled $K^*(CO_2^*)$, is expressed on the total pH scale:

$$K^*(CO_2^*) = (mH^+ + mHSO_4^-)\cdot mHCO_3^-/mCO_2^* \quad (3)$$

This can also be expressed as:

$$K^*(CO_2^*) = K(CO_2^*)\cdot[\gamma CO_2^*/(\gamma H^+\cdot\gamma HCO_3^-)]\cdot aH_2O \times \left(1 + mSO_4^{2-}\cdot\left[\gamma H^+\cdot\gamma SO_4^{2-}/\gamma HSO_4^-\right]/K(HSO_4^-)\right) \quad (4)$$

where $K(CO_2^*)$ and $K(HSO_4^-)$ are the thermodynamic values of the dissociation constants, aH_2O is the water activity, mSO_4^{2-} is the molality of free sulphate (i.e., excluding the amount taken up by HSO_4^-), and γ indicates an activity coefficient. The second expression above shows more clearly how $K^*(CO_2^*)$ depends on activity coefficients and therefore those interactions in the Pitzer model that can be expected to be important for the calculation of this quantity.

The variance contributions of $\ln(K(CO_2^*))$ and $\ln(K(HCO_3^-))$ to $\ln(K^*(CO_2^*))$, Fig. 1b, are both <10% of the total variance, and lower than that of $\ln(K(HSO_4^-))$, reflecting their lower uncertainties (Table 1). The assignment of the averaged values of Pitzer parameters (from paper (I), Appendix A) in place of those that are set to zero because they are unknown, does not introduce any variance contributions above 1%.

The uncertainty profile for the dissociation of HCO_3^- is shown in Fig. 1c. This stoichiometric dissociation constant can be written as:

$$K^*(HCO_3^-) = mH^{+(T)}\cdot mCO_3^{2-(T)}/mHCO_3^- \quad (5)$$

where superscript (T) indicates total molalities of both species. This expression expands to:

$$K^*(HCO_3^-) = (mH^+ + mHSO_4^-)\cdot(mCO_3^{2-} + mMgCO_3^0 + mCaCO_3^0 + mSrCO_3^0)/mHCO_3^- \quad (6)$$

where total carbonate ion consists of both free CO_3^{2-} and the amounts of the three ion pairs. Equation (6) can also be written in a similar way to Eq. (4), in terms of the thermodynamic equilibrium constant and activity coefficients (those of H^+ and CO_3^{2-} should both be on a total basis). The uncertainty contributions to the model calculated $\ln(K^*(HCO_3^-))$ in Fig. 1c are dominated, at about 30%, by the contribution of the thermodynamic value of the ion pairing constant for $MgCO_3^0$ (which was also found to have a strong influence on $pH^*_{T,m}$). As expected, interactions of Na^+ – the major cation of seawater – with CO_3^{2-} and HCO_3^- are also major contributors to the total variance. The small contribution of the ion pairing constant for $CaCO_3^0$ relative to that of $MgCO_3^0$ (despite the fact that they are assigned the same uncertainty) is mostly due to their relative concentrations in seawater (about 5:1, Mg^{2+}:Ca^{2+}). The introduction of averaged parameter values into the calculation, in place of those that are unknown and set to zero, increases the estimated standard deviation in $\ln(K^*(HCO_3^-))$ from 0.042 to 0.043. The cause of this is uncertainty contributions (2.5% of the variance) of parameters for the interactions of ion pair $CaCO_3^0$ with major ions Na^+ and SO_4^{2-}. (The ion Cl^- is the reference for all λ_{ni} Pitzer parameters for interactions between these carbonate ion pairs and cations and anions, hence $\lambda_{CaCO3,Cl}$ is zero by definition.) The unknown interaction between $MgCO_3^0$ and SO_4^{2-} adds about 1.3% to the total variance. We note that the interaction of this ion pair with Na^+ is quite poorly quantified (Section 2.1).

Figure 1d shows the uncertainty profile for the logarithm of the product $K^*(CO_2^*)\cdot K^*(HCO_3^-)$. This quantity can be measured directly (e.g., Prieto and Millero (2002), and Schockman and Byrne (2021)). Because the equilibrium relates the molalities of total H^+ ($H^{+(T)}$), CO_2^*, and $CO_3^{2-(T)}$ directly there are no uncertainty contributions that include the ion HCO_3^-:

$$K^*(CO_2^*)\cdot K^*(HCO_3^-) = [mH^{+(T)}]^2\cdot mCO_3^{2-(T)}/mCO_2^* \quad (7a)$$

$$= (mH^+ + mHSO_4^-)^2\cdot(mCO_3^{2-} + mMgCO_3^0 + mCaCO_3^0 + mSrCO_3^0)/mCO_2^* \quad (7b)$$

Consequently, comparisons with data for this quantity are a good test of the parameters for Na^+-CO_3^{2-} interactions in the model and the two thermodynamic equilibrium constants that together account for 44% of the estimated variance. The principal change in the uncertainty profile caused by the use of averaged parameter values in place of these that are unknown is the appearance of parameters $\lambda_{CaCO3,Na}$ and $\lambda_{CaCO3,SO4}$ (~2% of the total variance) and $\lambda_{MgCO3,SO4}$ (~1%). This is a similar result to that obtained for $\ln(K^*(HCO_3^-))$.

We have also calculated the uncertainty profile of the logarithm of the dissolved CO_2 molality, mCO_2^*, which is related to CO_2 fugacity for equilibrium between the gas and aqueous phases by $mCO_2^* = fCO_{2(g)}\cdot K_H(CO_2)/\gamma CO_2^*$, where prefix f denotes fugacity and K_H (mol kg^{-1} atm^{-1}) is the Henry's law solubility constant. This uncertainty profile is shown in Fig. S7 of the eighth document of the Supporting Information. The principal contributors to the estimated variance of 0.00167 in $\ln(mCO_2^*)$ are: Na^+-HCO_3^- interactions (30%); Cl^--HCO_3^- and related ternary interactions (26%); $\ln(K_f(MgCO_3^0))$ (15%), $\ln(K(HCO_3^-))$ (7.6%); Na^+-CO_3^{2-} interactions (6.6%), and $\ln(K(CO_2^*))$ (4.1%). This variance, and the uncertainty contributions to the calculated $\ln(mCO_2^*)$, are also a measure of the ability of the model to relate the speciation of dissolved carbonate to the equilibrium fugacity of CO_2 via the Henry's law constant of the gas. These results are quite similar to those for $\ln(K^*(HCO_3^-))$, with the exception that $\ln(K(HSO_4^-))$ does not contribute.

In the sections below we compare model predictions of the two carbonate dissociation constants and other properties with data from the sources listed in Table 2.

6.1.1. Variations of $\ln(K^*(CO_2^*))$ with salinity and temperature

In Fig. 2a we compare model predictions with measured values of $\ln(K^*(CO_2^*))$ (and empirical fits as functions of T and S) from five different sources as a function of salinity, for temperatures close to 25 °C. A similar comparison is made in part (b), as a function of temperature, for salinities close to 35. The shaded area in Fig. 2a represents the uncertainty envelope of the model prediction. At infinite dilution (zero salinity) this is equal to the uncertainty in $\ln(K(CO_2^*))$ only. This pair of plots captures, in a simple way, the concentration and temperature dependencies of deviations of the model from experimental measurements. Comparisons of data for all temperatures and salinities are shown in Fig. S1 in the eighth document of the Supporting Information. Note that results of Roy et al. (1993b) for salinity 5 are omitted from the plot because they appear to be in error (as noted by Millero et al., 2006).

First, the deviations of the measurements of Goyet and Poisson

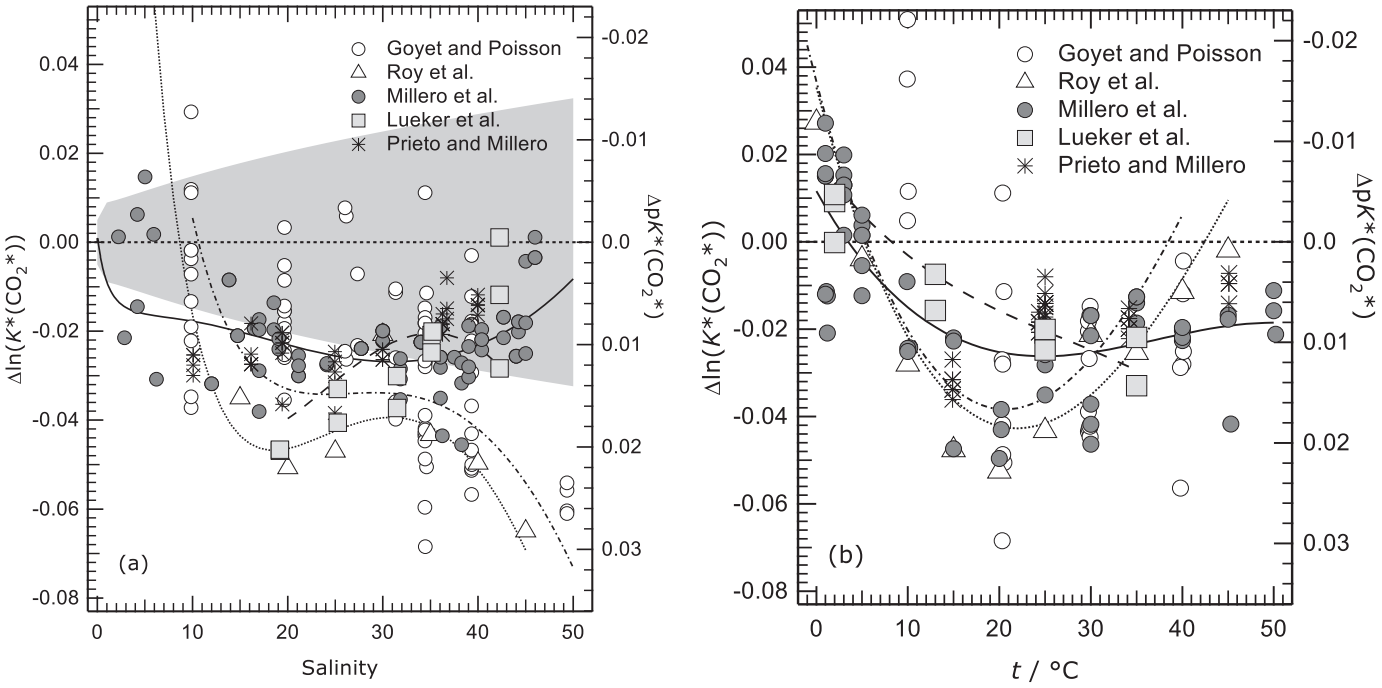

Fig. 2. The difference between measured and calculated values of $\ln(K^*(CO_2^*))$ (measured – calculated), for data from various sources. The equivalent scale in pK^* units is indicated on the right hand side. (a) Values at or close to 25 °C, plotted against salinity; (b) values at or close to salinity 35, plotted against temperature (t). Sources are as follows: open circle and dash-dot line – Goyet and Poisson (1989); triangle and dotted line – Roy et al. (1993b); shaded dot and solid line – Millero et al. (2006); shaded square and dashed line – Lueker et al. (2000); asterisk – Prieto and Millero (2002) (their table 7). The measurements of Roy et al. (1993b) are in artificial seawater not including F^- (and therefore on the total pH scale), those from other sources are in either natural seawater, or artificial seawater including F^- (and on the seawater pH scale). The shaded area in (a) indicates the estimated total uncertainty in the calculated values of $\ln(K^*(CO_2^*))$ at 25 °C, and is centered on the zero line.

(1989) from the model are not consistent with those of other data, and are more scattered. This behaviour is even more apparent in the comparisons for $\ln(K^*(HCO_3^-))$ (see next section), so they are not further considered. Deviations of other measurements from the model are almost all negative, but with a trend to smaller deviations at the highest and perhaps the lowest salinities. Such behaviour suggests that the cause is poor representation of solute interactions in the model, and the uncertainty profile in Fig. 1b shows that those for Na^+-HCO_3^- make the largest contribution to the uncertainty. These are taken from the study of Peiper and Pitzer (1982) of the EMFs and other literature data for solutions containing dissolved CO_2, $NaHCO_3$, Na_2CO_3 and chloride. The activity coefficients of $NaHCO_3$ that are obtained from these data, and which were used to determine the Na^+-HCO_3^- interaction parameters, depend upon assumptions regarding the activity coefficients of dissolved CO_2. The paper of Peiper and Pitzer predates the work of He and Morse (1993), which is the source of the CO_2^* and $B(OH)_3$ Pitzer interaction parameters used in this work. A comparison of the simple treatment of γCO_2^* in the analysis of Peiper and Pitzer with values obtained using the parameters of He and Morse suggests that a correction of the Na^+-HCO_3^- parameters i.e., a re-evaluation using γCO_2 from the work of He and Morse) is likely to bring the model into better agreement with the measurements at 25 °C.

Deviations of the model predicted values from measurements at different temperatures, Fig. 2b, also show a clear trend. The variation of the Na^+-HCO_3^- parameter values in the model with T also comes from the study of Peiper and Pitzer (1982) and therefore the same comments regarding model revisions apply.

Of the fitted curves shown in Fig. 2a,b that of Millero et al. (2006) appears to give the best representation of the data (excluding the results of Roy et al. (1993b) and Goyet and Poisson (1989)). This equation yields similar values to that of Millero (2010), as amended by Waters and Millero, 2013; Waters et al., 2014).

6.1.2. *Variations of ln(K*(HCO$_3^-$)) with salinity and temperature*

Figure 3 contains the same comparisons as above but for $\ln(K^*(HCO_3^-))$. The results of Goyet and Poisson (1989) and Roy et al. (1993b) deviate by up to about 0.1 in $\ln(K^*(HCO_3^-))$ from the other two studies, and are not further considered. At salinities above 10 the model agrees with the measurements at ~25 °C to within its estimated uncertainty but there are also clear trends in the deviations. The results for different temperatures, and salinity ~35, show a monotonic trend in the deviations which are greatest at the lowest temperature.

The uncertainty profile for $\ln(K^*(HCO_3^-))$ shows that the largest uncertainty contribution is that of $\ln(K_f(MgCO_3^0))$, as it also was for total pH. The value of this constant at 25 °C was obtained by Millero and Thurmond (1983) from measurements in solutions of NaCl containing low molalities of $MgCl_2$. The variation of $\ln(K_f(MgCO_3^0))$ with respect to temperature given in table II of Millero and Pierrot (1998) could not be found in the cited reference, but it is similar to values from Plummer et al. (1988) and from Nordstrom et al. (1990) at 25 °C.

Although the interaction parameter $\lambda_{MgCO3,Na}$ does not appear in the uncertainty profile in Fig. 1c, its value was estimated in this work from the results of Millero and Thurmond (1983) at only the single temperature of 25 °C (and for which deviations of model predicted $\ln(K^*(HCO_3^-))$ from the measurements are therefore relatively small). It is likely that a revised treatment of the variation with T of $\ln(K_f(MgCO_3^0))$ and the $MgCO_3^0$-Na^+ interaction will improve model predictions of the variation of $\ln(K^*(HCO_3^-))$ with temperature (Fig. 3b). The parameters for both Na^+-CO_3^{2-} and Na^+-HCO_3^- interactions are significant contributors to the uncertainty in the model calculated $\ln(K^*(HCO_3^-))$, at about the 10% to 15% level. Revisions to these sets of interaction parameters (both of which come from the study of Peiper and Pitzer (1982) which was discussed above) may improve the model with respect to the trend with salinity of the deviations shown in Fig. 3a.

Finally, we consider the deviations for salinities below 10 (Fig. 3a). These are large and negative, for a concentration range for which the

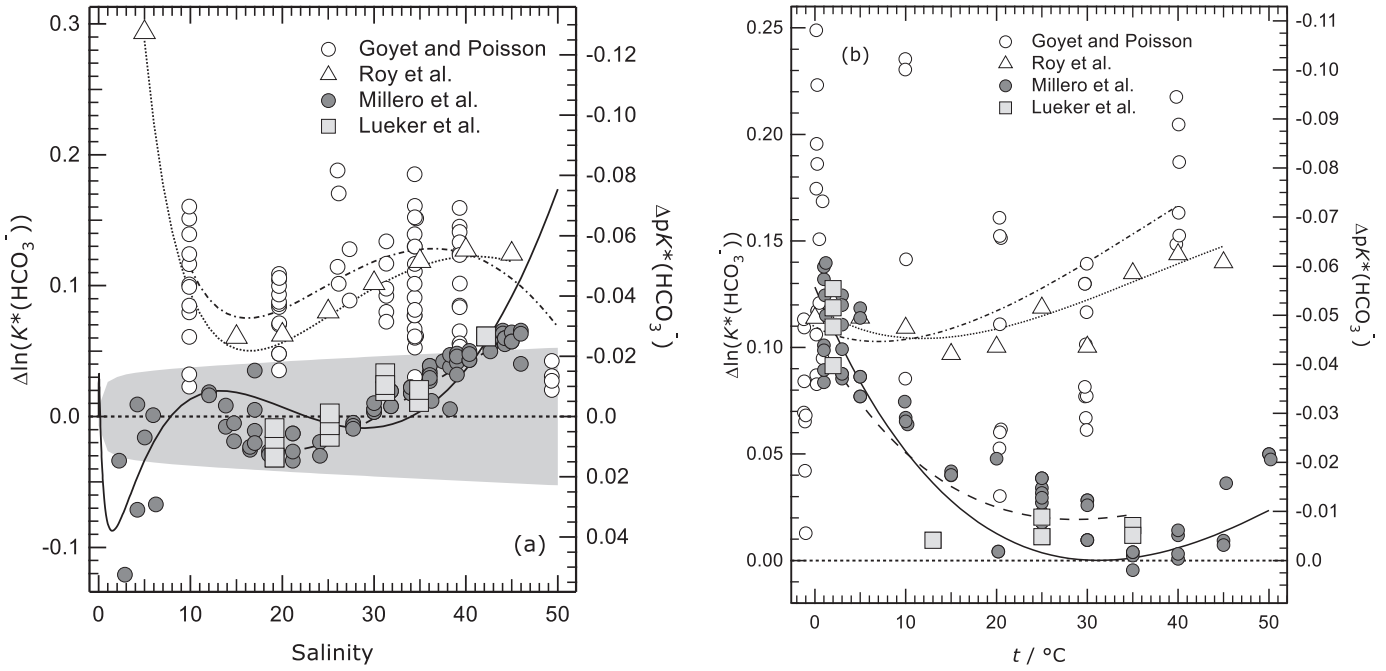

Fig. 3. The difference between measured and calculated values of $\ln(K^*(HCO_3^-))$ (measured – calculated), for data from various sources. (a) Values at or close to 25 °C, plotted against salinity; (b) values at or close to salinity 35, plotted against temperature (t). Sources are as follows: open circle and dash-dot line – Goyet and Poisson (1989); triangle and dotted line – Roy et al. (1993b); shaded dot and solid line – Millero et al. (2006); shaded square and dashed line – Lueker et al. (2000). The measurements of Roy et al. (1993b) are in artificial seawater not including F^- (and therefore on the total pH scale), those from other sources are in either natural seawater, or artificial seawater including F^- (and on the seawater pH scale). The shaded area in (a) indicates the estimated total uncertainty in the calculated values of $\ln(K^*(HCO_3^-))$ at 25 °C, and is centered on the zero line.

model would be expected to be subject to the smallest errors. The fitted equation of Millero et al. (2006) passes through these values, and shows a maximum negative deviation of about −0.09 in $\ln(K^*(HCO_3^-))$ at a salinity of about 1.5, and then a positive peak of about +0.03 extremely close to zero salinity. This behaviour is examined further in the eighth document of the Supporting Information, and found to be unphysical: that is to say, we believe the data at these very low salinities to be in error. Plots of deviations for all salinities and temperatures, shown in Fig. S4 of the same document indicate that this appears to be true at all the temperatures measured (from 0 to 40 °C).

Measurements of both $K^*(CO_2^*)$ and $K^*(HCO_3^-)$ at low salinities appear to be problematic, and it is likely that an improved model of carbonate dissociation equilibria in seawater – one that agrees with the data at all temperatures and at all higher salinities to within or close to experimental uncertainty – will yield more accurate values of the two constants for salinities below about 10 than have been determined to date.

6.1.3. *Variations of $\ln(K^*(CO_2^*)\cdot K^*(HCO_3^-))$ with salinity and temperature*

Model calculations of the logarithm of the product of the two stoichiometric equilibrium constants are compared in Fig. 4 with data from three studies (Prieto and Millero, 2002; Millero et al., 2006; and Schockman and Byrne, 2021). In the case of the Millero et al. (2006) study the products were calculated from the values of the individual constants listed in their table 4. Prieto and Millero (2002) and Schockman and Byrne (2021) measured $pK^*(CO_2^*) + pK^*(HCO_3^-)$ directly.

Results at ~25 °C are shown in Fig. 4a. It is clear that, first, the pattern of residuals is very similar to that for $\ln(K^*(HCO_3^-))$. Second, the data are widely scattered below salinity 10, and the fitted equations of Millero et al. (2006) (solid line) show the same anomalous behaviour as for $\ln(K^*(HCO_3^-))$. This is to be expected as the values shown on the plot were obtained from the equations for the two individual constants. The results in Fig. 4b, which shows residuals as a function of temperature at salinity ~35, are also very similar to those for $\ln(K^*(HCO_3^-))$. The principal contributors to the uncertainty in model calculated $\ln(K^*(CO_2^*)\cdot K^*(HCO_3^-))$, Fig. 1d, are $K(MgCO_3^0)$ and Na^+-CO_3^{2-} interaction parameters. (The H^+-Cl^- interaction is much less likely to be a cause of the observed differences between model and data because it is much better characterized.)

The inclusion in the model of averaged Pitzer parameter values for those that are unknown yields variance contributions of ~1% for $\lambda_{CaCO3,Na}$ and $\lambda_{CaCO3,SO4}$ (combined), and ~ 0.5% for $\lambda_{MgCO3,SO4}$. The plots of deviations for data at all temperatures and salinities, shown in Fig. S3 in the eighth document of the Supporting Information, are similar to those in Fig. 4a,b, except that the more comprehensive plot shows that the large positive deviations at the lowest temperatures are associated with salinities of about 20 and above.

6.2. *The stoichiometric solubility product of calcite, $CaCO_{3(s)}$*

The stoichiometric solubility product of calcite $K^*(CaCO_{3(s)})$ ($mol^2\,kg^{-2}$), in a solution in solubility equilibrium (i.e., saturated) with respect to the solid, is given by:

$$K^*(CaCO_{3(s)}) = \left\{ m{Ca^{2+}}^{(T)} \cdot m{CO_3^{2-}}^{(T)} \right\}_{sat.} \quad (8a)$$

$$= \left(m{Ca^{2+}} + m{CaCO_3}^o + m{CaF^+} \right) \cdot \left(m{CO_3^{2-}} + m{MgCO_3}^o + m{CaCO_3}^o + m{SrCO_3}^o \right) \quad (8b)$$

where the superscript (T) denotes total molalities that include those of various ion pairs, and the inclusion of the molality product within $\{\}_{sat.}$ indicates that it refers to the special condition of a saturated solution.

The value of $K^*(CaCO_{3(s)})$ can also be expressed in terms of the thermodynamic solubility product, and total activity coefficients of Ca^{2+} and CO_3^{2-}:

$$K^*(CaCO_{3(s)}) = K(CaCO_{3(s)}) / \left(\gamma{Ca^{2+}}^{(T)} \cdot \gamma{CO_3^{2-}}^{(T)} \right) \quad (9)$$

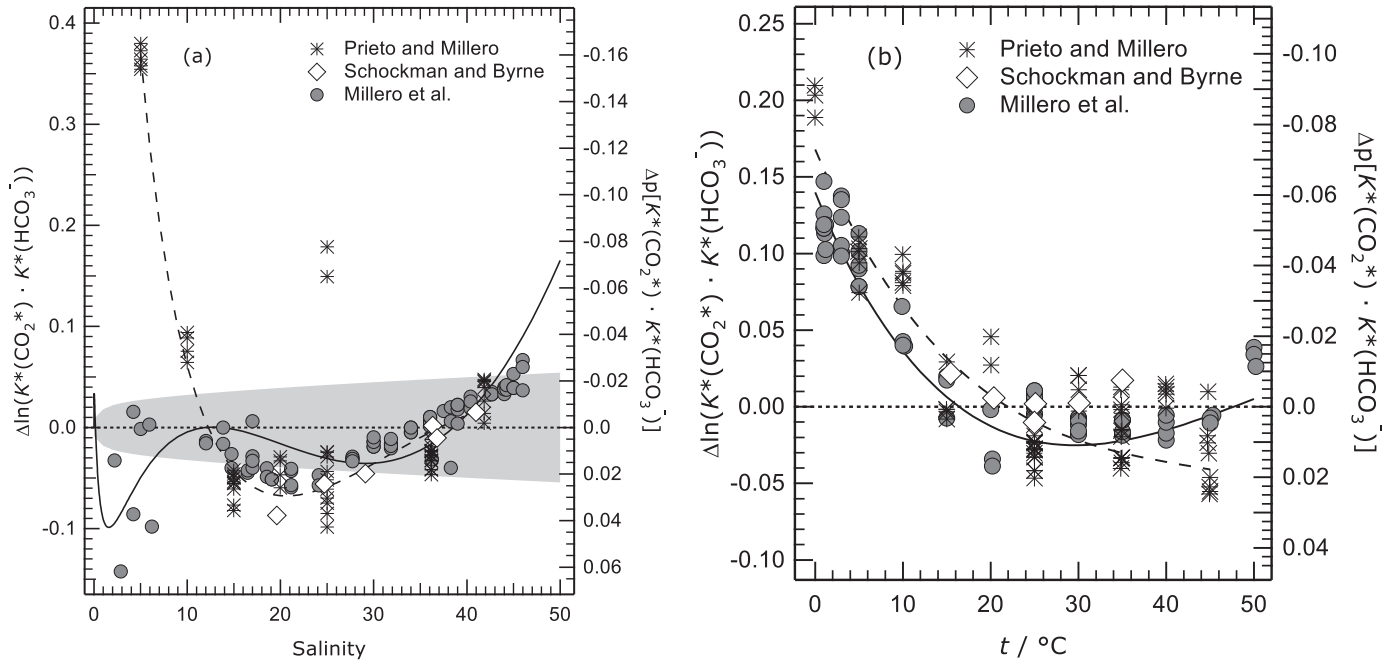

Fig. 4. The difference between measured and calculated values of $\ln(K^*(CO_2^*)\cdot K^*(HCO_3^-))$ (measured – calculated), for data from various sources. (a) Values at or close to 25 °C, plotted against salinity; (b) values at or close to salinity 35, plotted against temperature (t). Sources are as follows: asterisk and dashed line – Prieto and Millero (2002); diamond – Schockman and Byrne (2021); shaded dot and solid line – Millero et al. (2006). All measurements are in natural seawater. The seawater pH scale was used by Prieto and Millero (2002), and the total scale in the other two studies. The results of Schockman and Byrne (2021) (pH^0, their Table 1) were converted so that they are based upon the term $p(K_2^T e_2)$ in the expression for a spectrometric measurement of pH as follows: from Liu et al. (2011) (for salinities of 20 and above) and from Douglas and Byrne (2017) (for lower salinities). The shaded area in (a) indicates the estimated total uncertainty in the calculated values of $\ln(K^*(CO_2^*)\cdot K^*(HCO_3^-))$ at 25 °C, and is centered on the zero line.

where:

$$\gamma Ca^{2+(T)} = \gamma Ca^{2+} / \left(1 + mCO_3^{2-}\cdot K_f^*(CaCO_3^o) + mF^-\cdot K_f^*(CaF^+)\right) \quad (10)$$

$$\gamma CO_3^{2-(T)} = \gamma CO_3^{2-} / \left(1 + mMg^{2+}\cdot K_f^*(MgCO_3^o) + mCa^{2+}\cdot K_f^*(CaCO_3^o) + mSr^{2+}\cdot K_f^*(SrCO_3^o)\right) \quad (11)$$

In the model we use the expression of Plummer and Busenberg (1982) for the thermodynamic solubility product $K(CaCO_{3(s)})$. In the above equations for the total activity coefficients there are stoichiometric formation constants (K^*) of the same ion pairs that are found in Eq. (8). As an example, the expression for $K^*(MgCO_3^0)$ is given below:

$$K_f^*(MgCO_3^o) = mMgCO_3^o / \left(mMg^{2+}\cdot mCO_3^{2-}\right) \quad (12a)$$

$$= K_f(MgCO_3^o)\cdot\gamma Mg^{2+}\cdot\gamma CO_3^{2-} / \gamma MgCO_3^o \quad (12b)$$

where $K_f(MgCO_3^0)$ (kg mol^{-1}) is the thermodynamic value of the ion pairing constant and the molalities are those of the free species (i.e., not total values). In salinity 35 seawater we calculate that the proportions of the various dissolved carbonate species are as follows: 46% (free CO_3^{2-}), 42% ($MgCO_3^0$), 12% ($CaCO_3^0$), and 0.1% ($SrCO_3^0$). Free Ca^{2+} is >99.5% of the total Ca^{2+} molality.

Figure 5a shows the calculated uncertainty profile of $\ln(K^*(CaCO_{3(s)}))$ in salinity 35 seawater at 25 °C. By far the largest contributor to the total estimated variance is the thermodynamic equilibrium constant (about 55%), followed by that for ion pair $MgCO_3^0$ (about 15%). Pitzer parameters for Na^+-CO_3^{2-} interactions contribute about 10%. The use of averaged parameter values from Appendix A of paper (I) introduces variance contributions from parameters $\lambda_{CaCO3,Na}$ and $\lambda_{CaCO3,SO4}$ (about 1.3% of the total variance) and $\lambda_{MgCO3,SO4}$ (about 0.65% of the total variance).

Before comparing the model predicted $K^*(CaCO_{3(s)})$ to measured values, we carried out a series of calculations to examine the sensitivity of the activity coefficient product $\gamma Ca^{2+(T)}\cdot\gamma CO_3^{2-(T)}$ in Eq. (9) to changes in pH and total carbonate ion. In these calculations, all at salinity 35, the input HCO_3^- molality (0.0017803 mol kg^{-1}, from table 4 of Millero et al. (2008)) was reduced by factors ranging from 0.5 to 0.0135. For each of these reductions, the acidities of the solutions were adjusted to yield $pH^*_{T,m}$ ranging from about 7.5 to 8.5 or greater. We found that, in all these calculations, the value of the activity coefficient product varied by less than ±0.09%. This means that the stoichiometric molality product of total Ca^{2+} and CO_3^{2-} in seawater of a specified salinity and temperature saturated with respect to calcite is almost invariant with pH and total dissolved inorganic carbon. This is because the values of the stoichiometric ion pairing constants in Eqs. (10) and (11) are determined mainly by interactions with major seawater ions, and the two products in the denominator of Eq. (10) are both much less than unity and therefore have little influence on $\gamma Ca^{2+(T)}$.

Values of $K^*(CaCO_{3(s)})$, on an amount content basis (moles per kg of seawater), have been measured at three temperatures in seawaters of various salinities by Mucci (1983). We compare these values, after conversion to a molality basis, with the predictions of the model in Fig. 5b. Although the variation of $\ln(K^*(CaCO_{3(s)}))$ with temperature is reproduced quite well by the model, especially for salinity 35, there is a positive trend in the deviations with salinity which lies outside of region of uncertainty of the prediction. It seems likely that the deviations are related to two elements of the model: the value of $K(CaCO_{3(s)})$, because otherwise it would be expected that deviations in Fig. 5b would tend to zero as salinity decreases; and also the formation of ion pair $MgCO_3^0$ that accounts for up to about half of total CO_3^{2-}. In order to improve the model it will be necessary to examine the derivation of the value of $K(CaCO_{3(s)})$ – which is itself dependent on the model used by Plummer and Busenberg (1982) – and the formation of $MgCO_3^0$ and its interactions with other ions.

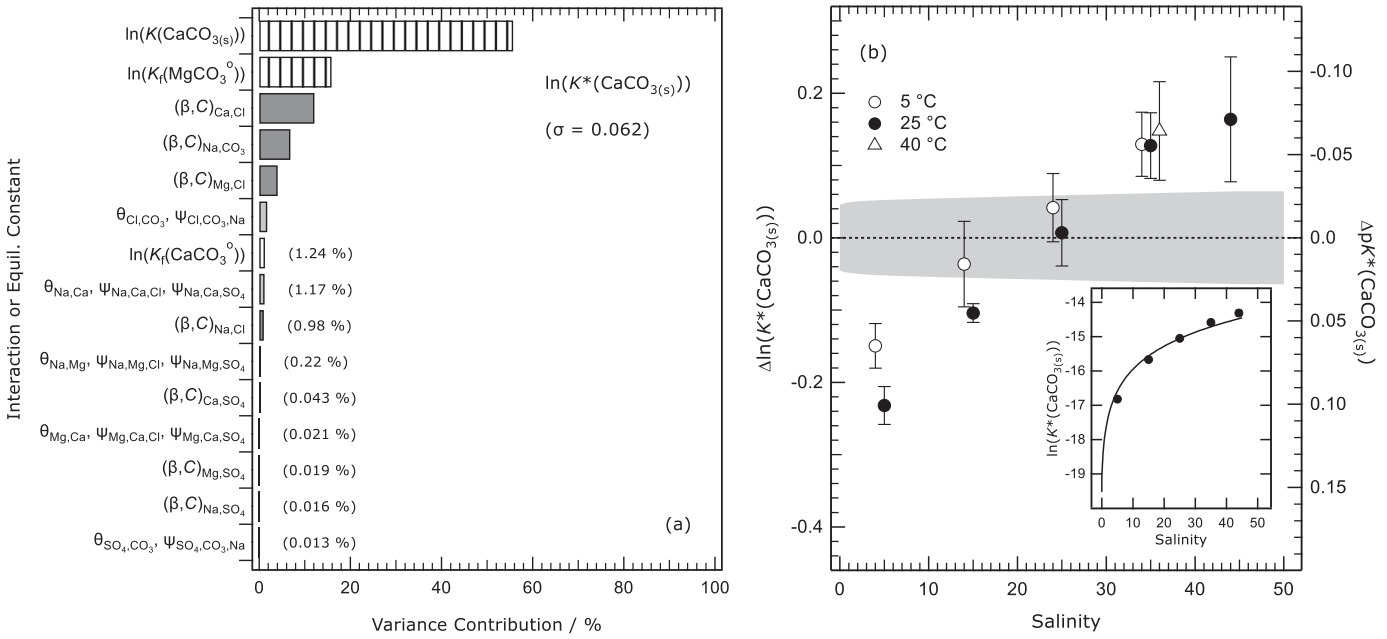

Fig. 5. (a) Percentage contributions of individual Pitzer model interactions, and equilibrium constants, to the variance of calculated ln($K^*(CaCO_{3(s)})$) in salinity 35 seawater at 25 °C. The parameters associated with each of the interactions are listed down the left-hand sides, and contributions of about 1% and below are noted on the plots. Symbols K(*species*) and K_f(*species*) denote the thermodynamic equilibrium constants of the named solute species, as defined in Table 1. Only the fifteen largest contributions are shown. The standard uncertainty of the calculated quantity is given on the plot. (b) Differences between measured and calculated ln($K^*(CaCO_{3(s)})$) in artificial seawater as a function of salinity, at three different temperatures (indicated on the plot). The data are from table 3 of Mucci (1983). The shaded area indicates the estimated total uncertainty in the calculated values at 25 °C, and is centered on the zero line. Inset: measured (points) and calculated (solid line) values at 25 °C only.

6.3. *Borate equilibria*

Stoichiometric dissociation constants of boric acid have been determined by Dickson (1990) from EMFs of Harned cells containing artificial seawater and borax. Fig. 6a shows the uncertainty profile of the model calculated value of ln($K^*(B(OH)_4^-)$) in salinity 35 seawater at 25 °C. The stoichiometric dissociation constant $K^*(B(OH)_4^-)$, on a total hydrogen ion basis, is given by:

$$K^*(B(OH)_4^-) = K(B(OH)_4^-)\cdot\left(\gamma B(OH)_4^- / \gamma B(OH)_3\right)\cdot(1/aH_2O) \times \left[\gamma H^+ / \left(1 + mSO_4^{2-} / K^*(HSO_4^-)\right)\right] \quad (13)$$

where $K(B(OH)_4^-)$ is the thermodynamic dissociation constant, and $K^*(HSO_4^-)$ is the stoichiometric dissociation constant of HSO_4^- at the salinity and temperature of interest.

The greatest uncertainty contributions to the calculated value ln($K^*(B(OH)_4)^-$) in Fig. 6a, apart from the parameters for H^+-Cl^- interactions (which are well characterized), are those for Na^+-$B(OH)_4^-$, Cl^--$B(OH)_4^-$ and some related ternary interactions, and the thermodynamic dissociation constant of HSO_4^-. Interactions involving SO_4^{2-} and HSO_4^- are present in the uncertainty profile because of their influence on the value of $K^*(HSO_4^-)$. The Na^+-$B(OH)_4^-$ parameters in the model are from Simonson et al. (1987), who measured EMFs of NaCl solutions containing about 0.025 mol kg^{-1} of borate ion and boric acid. Although these molalities are quite low, it appears likely that some polyborate formation occurred. Simonson et al. (1987) discuss this, and also carried out test calculations in which the formation of two polyborate species were included. It was found that the fitted Pitzer interaction parameters were not strongly affected, but that the calculation was sensitive to assumptions made concerning the activity coefficients of the polyborate anions. It therefore seems likely that the uncertainty associated with the Na^+-$B(OH)_4^-$ interaction parameters in the model is larger than has been assumed.

The presence of the Mg^{2+}-$B(OH)_4^-$ interaction (at about the 1% level in Fig. 6a) deserves special mention. This very strong interaction can alternatively be treated as ion pair formation (and the same is true of Ca^{2+}-$B(OH)_4^-$). The parameters for these interactions were obtained from EMF measurements by Simonson et al. (1988), who state that the standard errors of fit were 0.65 mV for the solutions containing Mg^{2+}. This value is comparatively large, about an order of magnitude larger than the precision of a typical Harned cell measurement of EMF. Also important is the fact that polyborate formation is likely in their solutions, which contain very similar borate and boric acid molalities to those studied by Simonson et al. (1987). Simonson et al. (1988) compare their results with those of Felmy and Weare (1986) and Hershey et al. (1986), and discuss the difficulties of modelling these solutions. They also point out that the coupling of parameters and the inability to determine values of some mixing terms increases uncertainty in calculated quantities far from experimental conditions. The uncertainty contribution of the strong Mg^{2+}-$B(OH)_4^-$ interaction to modelled ln($K^*(B(OH)_4^-)$) seems likely to be much greater than indicated in Fig. 6a, and requires further study.

Model calculated ln($K^*(B(OH)_4^-)$) are compared with values determined by Dickson (1990) (his table 3) in Fig. 6b,c. The differences between the two (Fig. 6c) greatly exceed the estimated uncertainties. This suggests, first, there may indeed be errors in the Na^+-$B(OH)_4^-$ and Mg^{2+}-$B(OH)_4^-$ interaction parameters for the reasons given above. Second, it is possible that polyborate formation in the solutions measured by Dickson (1990) may have influenced the values of ln($K^*(B(OH)_4^-)$) derived from the data, although it is not clear that this would be so given that they are obtained by extrapolation to an artificial seawater medium containing no added borates. There is a clear negative trend in the deviations with salinity (Fig. 6c), and also variations with temperature. It is noted that the deviations do not tend to zero at zero salinity for the highest temperatures, which is unexpected given that the model uses the same values of the thermodynamic dissociation constant as did Dickson (1990) in his analysis. Dickson stated that there were some systematic deviations of the ln(K^*) in his table 3 from the fitted equation used to

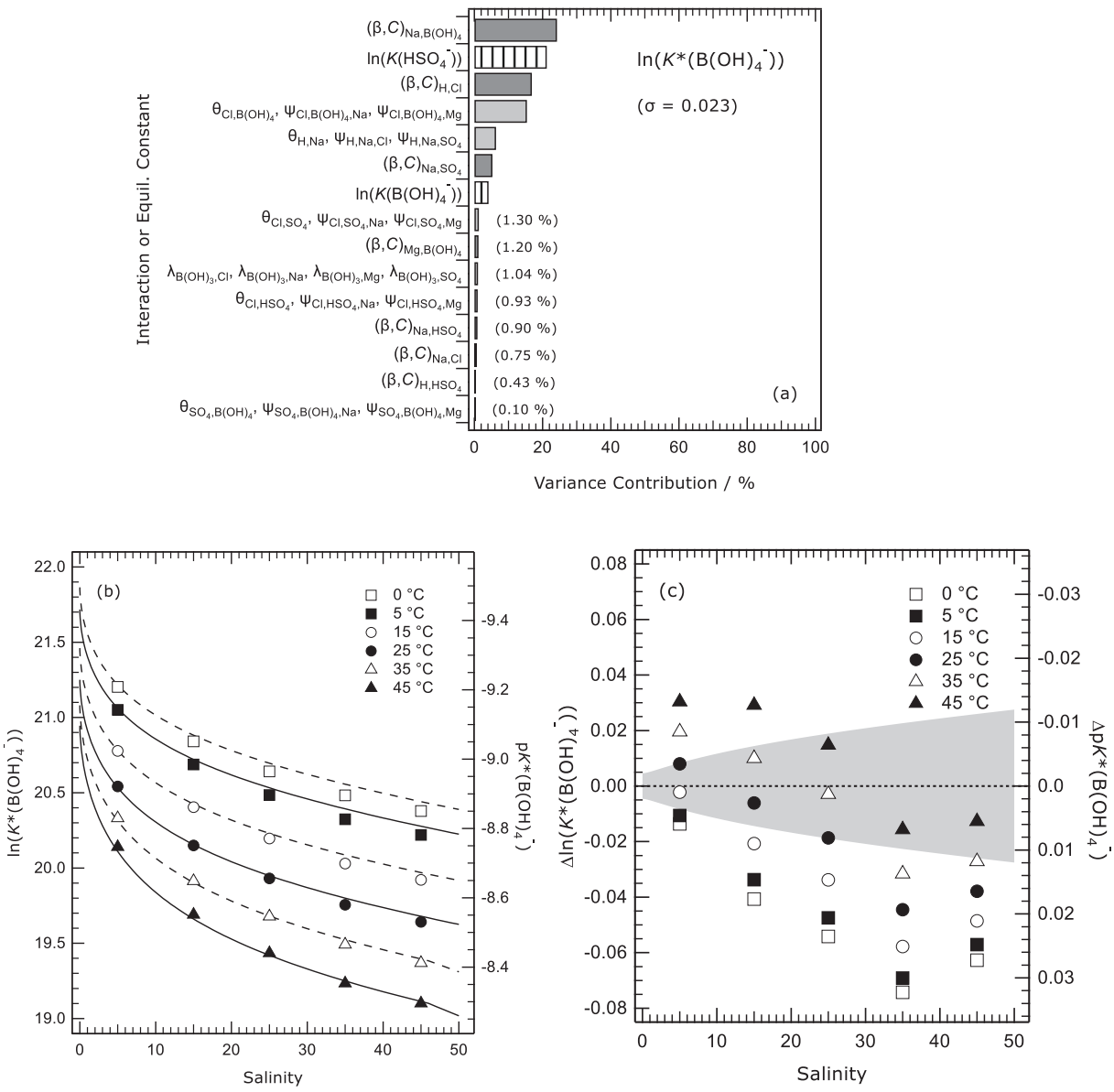

Fig. 6. (a) Percentage contributions of individual Pitzer model interactions, and equilibrium constants, to the variance of the $\ln(K^*(B(OH)_4^-))$ in salinity 35 seawater at 25 °C. The parameters associated with each of the interactions are listed down the left-hand side, and contributions of <1% are noted on the plot. Symbol $K(B(OH)_4^-)$ denotes the thermodynamic dissociation constant of $B(OH)_4^-$. Only the fifteen largest contributions are shown. The standard uncertainty of the calculated $\ln(K^*(B(OH)_4^-))$ is given on the plot. (b) Measured and calculated stoichiometric dissociation constants of $B(OH)_4^-$, $\ln(K^*(B(OH)_4^-))$, as a function of salinity. The data are from table 3 of Dickson (1990), and the calculations are for seawater of the composition given in table 4 of Millero et al. (2008). Symbols: values for six different temperatures, as indicated on the plot. Lines: calculated using the present model. (c) The differences between measured and calculated $\ln(K^*(B(OH)_4^-))$ (the same data as in panel (b)). The shaded area indicates the estimated total uncertainty in the calculated values of $\ln(K^*(B(OH)_4^-))$ at 25 °C, and is centered on the zero line.

represent them (his eq. (23)), which may be relevant to this point.

The EMFs of the Harned cells studied by Dickson (1990) are related to the activity product of free H^+ and Cl^- in the solutions by:

$$(E - E^0) = -(RT/F)\cdot\ln(aH^+\cdot aCl^-) \quad (14)$$

where E (V) is the measured EMF, E^0 (V) is the standard EMF of the cell at the temperature T (K) of interest, R (8.31446 J mol^{-1} K^{-1}) is the gas constant, F (96,485.337 C mol^{-1}) is the Faraday constant, and prefix a denotes activity. Replacing aH^+ in the equation by a term including the constant for $B(OH)_4^-$ dissociation (Table 1), we obtain:

$$(E - E^0) = -(RT/F)\cdot\left[\ln(aCl^-) + \ln\left(aB(OH)_3\cdot aH_2O/\left(aB(OH)_4^- \cdot K(B(OH)_4^-)\right)\right)\right] \quad (15)$$

The solutions measured by Dickson (1990) contain similar borate molalities to those studied by Simonson et al. (1988). We therefore carried out calculations to examine the possible influence of the formation of polyborate species by including in the model the primary polyborate species ($B_3O_3(OH)_4^-$) obtained by Felmy and Weare (1986). The equilibrium constant, at 25 °C, was obtained from the values of μ^o/RT in their table 2, and interaction parameters from their tables 3–5. First, we compared measured EMFs with those calculated using the present model (without the additional species) and found there to be a strong dependence of the differences, $\Delta(E - E^0)$, on the total borate molalities. The inclusion of the species $B_3O_3(OH)_4^-$ greatly reduced this dependence at salinities up to 25, and also reduced the magnitude of the deviations. For example, in salinity 5.01 artificial seawater, at 25 °C, values of $\Delta(E - E^0)$ calculated using the present model ranged from about +0.3 to +1.5 mV. The inclusion of $B_3O_3(OH)_4^-$ formation reduced this range to about +0.2 to +0.55 mV. Similar improvements were

obtained at salinities 15 and 25, but less so at salinity 35 and particularly salinity 45. These results suggest that it is necessary to include one or more polyborate species in order to predict accurately the EMFs of these solutions, and those measured by Simonson et al. (1987, 1988) which contain similar borate and boric acid molalities. The calculated $pH^*_{T,m}$ of seawater solutions is insensitive to borate equilibrium, and Na^+-$B(OH)_4^-$ interactions contribute <1% to the estimated variances, Fig. 1a. However, further investigation of both polyborate formation and interactions of $B(OH)_4^-$ with Na^+ and Mg^{2+}, in the thermodynamic studies from which borate interaction parameters are obtained (and which involve much higher borate concentrations than seawater), are likely to be worthwhile to improve the model.

6.4. The ion product of water

The ion product of water, $K^*(H_2O)$, in seawater has been determined by Dickson and Riley (1979) by potentiometric titration from salinity 10.43 to 47.78, at different temperatures. The seawater scale is used for H^+ ion concentration. The uncertainty profile, and comparisons with the model, are shown in Fig. 7.

The uncertainty profile is dominated by the Mg^{2+}-Cl^- interaction, and the thermodynamic equilibrium constants $K_f(MgOH^+)$, $K(H_2O)$, and $K(HSO_4^-)$. Relatively few interactions between $MgOH^+$ and other ions have been characterized, and the use of averaged values of parameters from Appendix A of paper (I) in the place of those that are unknown yields parameter $\theta_{Na,MgOH}$ as the one with the largest uncertainty

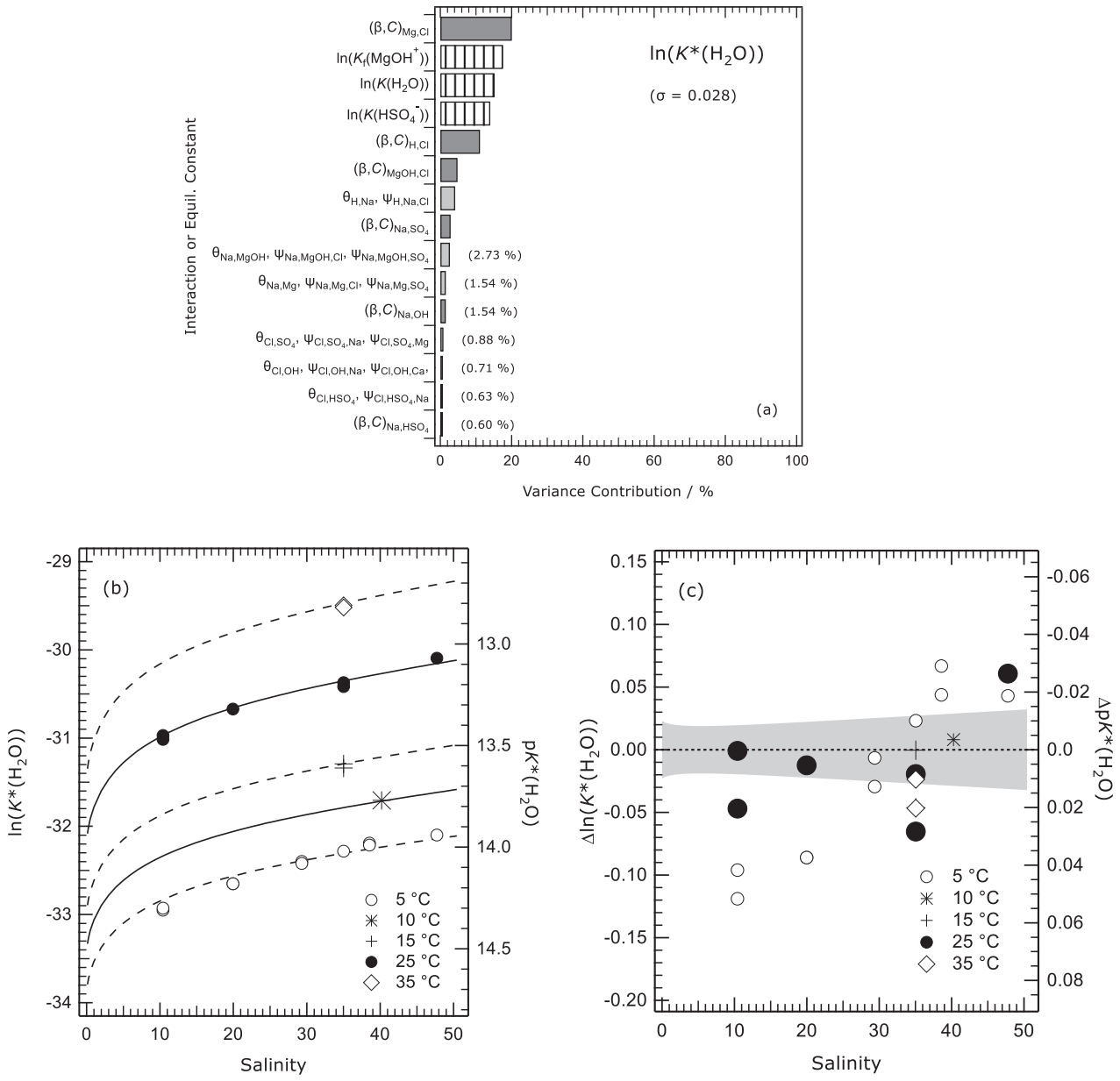

Fig. 7. (a) Percentage contributions of individual Pitzer model interactions, and equilibrium constants, to the variance of calculated $\ln(K^*(H_2O))$ in salinity 35 seawater at 25 °C. The parameters associated with each of the interactions are listed down the left-hand sides, and contributions of about 2% and below are noted on the plots. Symbols *K*(*species*) and K_f(*species*) denote the thermodynamic equilibrium constants of the named solute species, as defined in Table 1. Only the fifteen largest contributions are shown. The standard uncertainty of the calculated quantity is given on the plot. (b) Differences between measured and calculated $\ln(K^*(H_2O))$ in artificial seawater as a function of salinity, at five different temperatures (indicated on the plot). The data are from table II of Dickson and Riley (1979), and the H^+ molality in the ion product is the total on the seawater scale (the artificial seawater used in the experiments includes F^-). The shaded area indicates the estimated total uncertainty in the calculated values of $\ln(K^*(H_2O))$ at 25 °C, and is centered on the zero line.

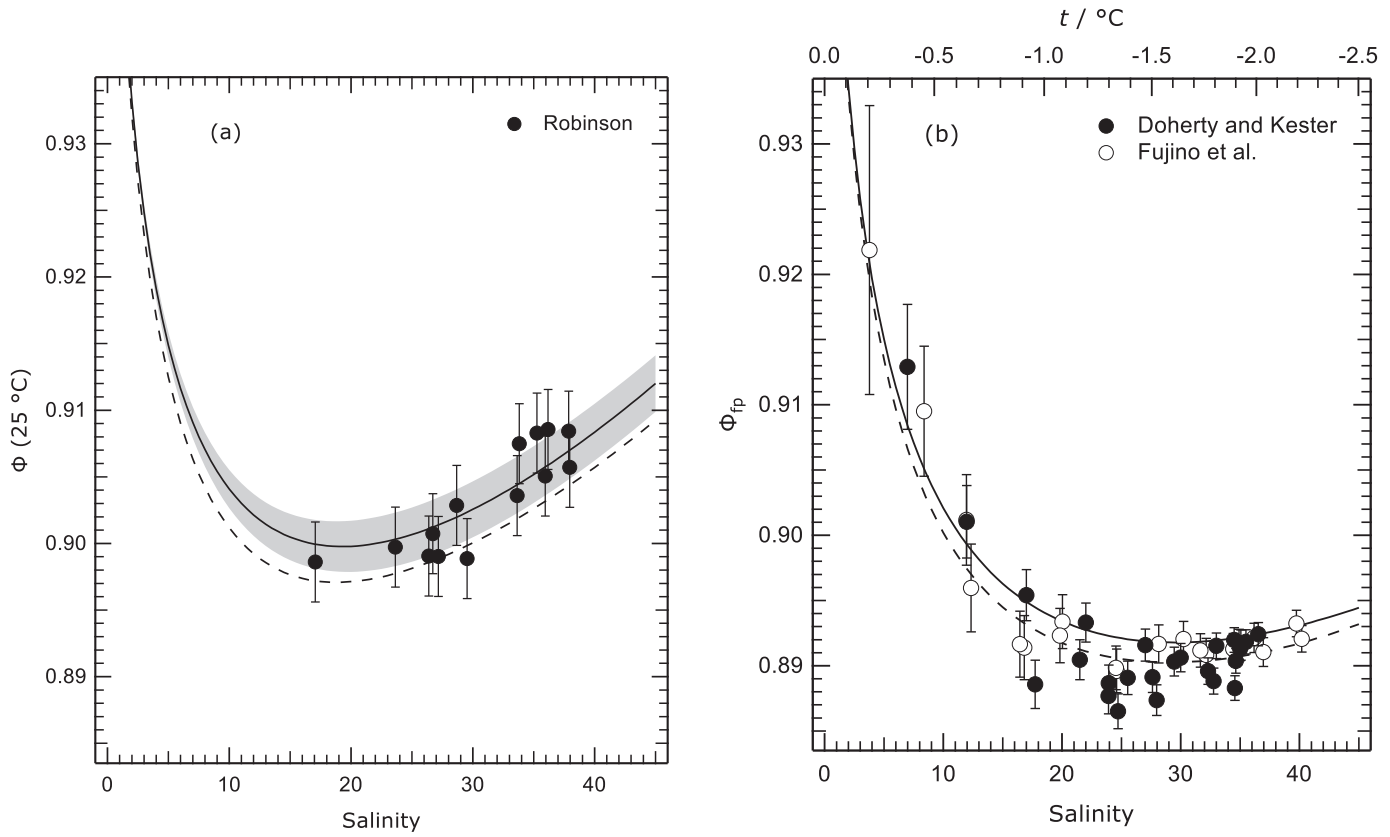

Fig. 8. (a) Osmotic coefficients (ϕ) of seawater at 25 °C. Symbol: data of Robinson (1954). Lines: solid – the present model; dashed – TEOS-10 (Feistel, 2008). The error bars are an assumed uncertainty of ±0.003, which is generally typical of an isopiestic experiment. The shaded area indicates the estimated uncertainty of the model prediction. (b) Osmotic coefficients of seawater at its freezing temperature (ϕ_{fp}), and plotted against salinity (and freezing temperature *t*, on the top axis). Symbols: open circle – Fujino et al. (1974); dot – Doherty and Kester (1974). The lines have the same meanings as in (a). The error bars correspond to experimental uncertainties of ±0.002 °C (Doherty and Kester, 1974), and ± 0.0025 °C (Fujino et al., 1974) in the freezing temperature.

contribution (24%), and 8% for the ($\beta^{(0,1)}_{ca}$, $C^{(0,1)}_{ca}$) parameters describing the $MgOH^+$-SO_4^{2-} interaction. The deviation plot, Fig. 7c, shows that while results are satisfactory at 25 °C, there is a clear trend with salinity at 5 °C. A possible cause of this is the fact that the parameters for the $MgOH^+$-Cl^- interaction are known only at 25 °C unlike the other interactions and equilibrium constants at higher positions in the uncertainty profile in Fig. 7a.

6.5. The osmotic coefficient of seawater

Calculations of the osmotic coefficient (ϕ) of seawater are a test of the accuracy of the model in representing interactions between the major ions of seawater: Na^+, Mg^{2+}, Cl^-, and SO_4^{2-}. A calculated uncertainty profile for the osmotic coefficient of salinity 35 seawater (not shown) yields the following contributions to the total variance: Na^+-Cl^-, 86%; Mg^{2+}-Cl^-, 8%; Na^+-SO_4^{2-}, 2%; Na^+-Mg^{2+} and related ternary interactions, 2%; Cl^--SO_4^{2-} and related ternary interactions, 2%. The osmotic coefficient of an aqueous solution is related to its water activity by:

$$\ln(aH_2O) = (M_W/1000)\cdot\phi\cdot\Sigma_i\, m_i \qquad (16)$$

where M_w (g mol^{-1}) is the molar mass of water and the summation is over the molalities of all solute species i. In order to obtain a value of $\Sigma_i\, m_i$ for seawater we first determined a hypothetical mean molar mass of seawater of 31.4038 g for the listed speciation of salinity 35 seawater in table 4 of Millero et al. (2008). From this value, and the absolute salinity of any seawater sample, it is then possible to calculate a corresponding seawater molality. All osmotic coefficients calculated by the model, for which the solute speciation will differ (for the minor species) from that in the table of Millero et al., were converted to be on the same fixed speciation basis by recognizing that the osmolalities (the product involving the final two terms in Eq. (16)) have the same value on either basis.

We first calculated seawater osmotic coefficients from the results of isopiestic measurements of Robinson (1954), using the model of Archer (1992) to calculate osmotic coefficients of the NaCl reference solutions. The results are compared with the model, and with values calculated using the equation of state for seawater TEOS-10 (Feistel, 2008), in Fig. 8a. There is excellent agreement with the data at this temperature. The predictions of TEOS-10 are lower, but also agree with this single dataset satisfactorily.

Next, water activities at the freezing temperature of seawater were calculated from measured freezing point depressions (Doherty and Kester, 1974; Fujino et al., 1974) using standard relationships (Klotz and Rosenberg, 1972), and then converted to osmotic coefficients at the freezing temperature (ϕ_{fp}) using Eq. (16) above. These values are compared with model predictions, and with TEOS-10, in Fig. 8b. In this case the TEOS-10 predictions are in slightly better agreement with the data, suggesting that the model may not represent major ion interactions (chiefly Na^+-Cl^- and Mg^{2+}-Cl^-) close to 0 °C quite as well as it does at 25 °C.

7. Recommendations for future work

Here we outline those elements of the model – equilibrium constants and Pitzer activity coefficient parameters – likely to need revision in order to improve agreement with the measured speciation to within, or close to, experimental uncertainty. The profiles shown in Section 6

identify the major contributors to the variances of model predictions of $pH^*_{T,m}$, carbonate and borate equilibria, calcite saturation, and the ionic product of water. These contributors are identified in Table 3 together with the predicted quantities for which they are most important. We classify them according to whether their variance contributions in the simulations for salinity 35 and 25 °C are >20%, 10–20%, 5–10%, or 2–5% of the totals.

Table 3, and the uncertainty simulations on which it is based, is intended as guide to assist future data analyses and experiments to improve the model for the calculation of total pH, and the equilibria listed in the table, for natural waters containing the ions of seawater. It is important to bear in mind the following limitations:

(i) The uncertainty simulations are for 25 °C only. Some interaction parameters are available only for this temperature, and their use for calculations at other temperatures may introduce much larger errors into a calculated quantity than is suggested by their positions in the uncertainty profile. An example is the $MgOH^+$-Cl^- interaction in the calculation of $\ln(K^*(H_2O))$.

(ii) Basing the uncertainty estimations on the assumption of datasets of osmotic coefficients of typical quality does not take into account the errors and uncertainties of the real datasets(s) used, the uncertainties associated with different types of data (for example EMFs as compared to osmotic coefficients, see paper (I)), nor the number of such datasets from which a set of interaction parameters is derived. For example, there have been numerous studies of the thermodynamic properties of aqueous HCl and solutions containing the principal electrolytes of seawater, but the parameters for the interaction of Na^+ and $B(OH)_4^-$ are largely based upon a single EMF study.

(iii) Pitzer parameters in the model that have been drawn from different studies of the many single solute solutions and simple mixtures comprising the ions of seawater may not be self-consistent. Common examples are the ternary interaction parameters $\theta_{ii'}$ and $\psi_{ii'j}$ that depend on those used to calculate the binary cation-anion interactions in the solutions. The effect of the inconsistencies that can arise when $\theta_{ii'}$ and $\psi_{ii'j}$ are used with different sets of cation-anion parameters is not taken into account here. An important example in the model, of a similar kind, is the

Table 3
Percentage contributions of the principal interactions and equilibrium constants to the variances of $pH^*_{T,m}$ and various stoichiometric constants, in salinity 35 seawater at 25 °C.

Interaction or Eql. Constant	$pH^*_{T,m}$	$K^*(CO_2^*)$	$K^*(HCO_3^-)$	$K^*(CO_2^*) \times K^*(HCO_3^-)$	mCO_2^*	$K^*(CaCO_{3(s)})$	$K^*(H_2O)$	Borate (EMF) [a]
$K(CO_2^*)$		5		2	2			
$K(HCO_3^-)$		5	2		5			
$K(CaCO_{3(s)})$						**20**		
$K(B(OH)_4^-)$								5
$K(H_2O)$							**10**	
$K(HSO_4^-)$	**10**	**10**	5	**10**			**10**	
$K_f(MgOH^+)$							**10**	
$K_f(MgCO_3^0)$	**20**		**20**	**20**	**10**	**10**		
$K_f(CaCO_3^0)$			2	2				
$(\beta,C)_{H,Cl}$	5	**10**	2	**10**			**10**	
$(\beta,C)_{Na,Cl}$								**20**
$(\beta,C)_{Mg,Cl}$	5		5		2	2	**20**	
$(\beta,C)_{Ca,Cl}$						**10**		
$(\beta,C)_{Na,SO4}$		2		2			2	
$(\beta,C)_{Na,HCO3}$	5	**20**	**10**		**20**			
$(\beta,C)_{Na,CO3}$	**10**		**10**	**10**	5	2		
$(\beta,C)_{Na,B(OH)4}$								**20**
$(\beta,C)_{Mg,B(OH)4}$								2
$(\beta,C)_{MgOH,Cl}$							5	
$(\theta,\psi)_{H,Na,X}$ [b]	2	2		5			2	
$(\theta,\psi)_{Cl,HCO3,M}$ [c]	5	**20**	5		**20**			
$(\theta,\psi)_{Cl,CO3,M}$ [c]	2		2		2	2		
$(\theta,\psi)_{Na,MgOH,X}$ [b]							2	
$(\theta,\psi)_{Cl,B(OH)4,M}$ [c]								**20**
Other interactions [d]								
$(\beta,C)_{MgOH,SO4}$							5	
$(\theta,\psi)_{Na,MgOH,X}$ [e]							**20**	
$\lambda_{B(OH)3,M}$ [f]	2							
$\lambda_{CaCO3,I}$ [g]			2	2		2		

Notes: This table summarises the results of the uncertainty profiles shown in the figures in Section 6. Entries indicate that the percentage variance contribution of the interaction or ln(equilibrium constant) (left hand side) to the indicated quantity exceeds the value given. Hence, for example, the contribution of $\ln(K_f(MgOH^+))$ to the total variance of the natural log of the stoichiometric constant $K^*(HCO_3^-)$ is ≥20%. Contributions of below 2% are not listed (and the entries in the table are blank in this case).

[a] The stoichiometric dissociation constant of $B(OH)_4^-$ is determined from measurements of the EMFs of artificial seawater solutions containing borax, and it is therefore uncertainty contributions to the calculated EMF of such a solution (Fig. 6a) that are listed here.

[b] These interactions are $\theta_{cc'}$ between the two indicated cations, and $\psi_{cc'X}$ where X is an anion (usually in the order of concentration in seawater: Cl^-, SO_4^{2-}, etc.). The first two or three $\psi_{cc'X}$ can be found in the figure for the uncertainty profile for the quantity of interest.

[c] The same as for note b above, except for anion-anion, and anion-anion-cation interactions, where M is a metal cation (usually in the order of concentration in seawater: Na^+, Mg^{2+}, Ca^{2+}, etc.).

[d] Parameters that are normally set to zero in the model, but may have non-zero values. They have been assigned averaged values and associated variances (from Appendix A in paper (I)) for these calculations.

[e] Anions X are Cl^- and SO_4^{2-}.

[f] Cations M are Mg^{2+} and Ca^{2+}.

[g] Ions I are Na^+ and SO_4^{2-}.

Na^+- $B(OH)_4^-$ and very strong Mg^{2+}- $B(OH)_4^-$ interactions: ternary interaction parameters involving $B(OH)_4^-$ and these two cations are not the same as used in their determination, which is likely to introduce errors into model predictions. The identification of inconsistencies of these and other kinds, not all of which may be important, requires examination of the studies in which they have been determined. The uncertainty profiles presented in this work can be used to assess the relative contribution of a parameter to the quantity of interest, and therefore whether revision to obtain an improved value is likely to be worthwhile. The most important parameters are generally those that include, as one or more interacting species, the major ions of seawater (Na^+, Cl^-, Mg^{2+} and SO_4^{2-}) because they have the highest molalities. Sources of all parameters and equilibrium constants are listed in the Supporting Information.

Next, we briefly review some aspects of the equilibrium constants in the model that relate to uncertainties in model predictions and, separately, the model representation of the activity coefficients for the various equilibria.

7.1. Thermodynamic equilibrium constants

It is known that the value for $K(HSO_4^-)$ requires revision, together with the related Pitzer parameters for H^+-SO_4^{2-} and H^+-HSO_4^- interactions (see paper (I)). Revisions to $K(HSO_4^-)$ (probably of the order of 3% at 25 °C) should improve predictions of $pH^*_{T,m}$, $K^*(CO_2^*)$, $K^*(H_2O)$, and $K^*(HCO_3^-)$. The trend in the deviations between measured and calculated $\ln(K^*(B(OH)_4^-))$ in artificial seawaters containing borax, as salinity tends to zero (Fig. 6c), suggests that the derivation of $\ln(K^*(B(OH)_4^-))$ may also be worth reviewing, although the behaviour of these solutions is complicated by the formation of polyborate species and the very strong interaction of $B(OH)_4^-$ with Mg^{2+}. We have not critically examined the thermodynamic equilibrium constants for water dissociation, or those for carbonate dissociation.

The ion pairing constant $K_f(MgCO_3^0)$ is a key contributor to the total estimated uncertainties of five of the quantities in Table 3. Its value at 25 °C was determined by Millero and Thurmond (1983), and the variation with temperature seems likely to be based upon an analysis of solubility data but we have been unable to find this described in the literature. We note that the constant slope of the change in $\log_{10}(K_f(MgCO_3^0))$ with respect to temperature of 0.0066154 (table II of Millero and Pierrot (1998)) is close to that of Plummer et al. (1988) (0.006234 at 25 °C) and of Nordstrom et al. (1990) (0.00667).

The value of $K_f(CaCO_3^0)$ in the model is slightly greater than $K_f(MgCO_3^0)$, which would not be expected simply from ion size considerations. However, formation of this ion pair is less than $MgCO_3^0$ in seawater because the Ca^{2+} concentration is lower than that of Mg^{2+}. It has been assigned the same variation with temperature as $K_f(MgCO_3^0)$ by Millero and Pierrot (1998), although the reason for this isn't clear. In the Pitzer model of Plummer et al. (1988) the expression for $K_f(CaCO_3^0)$ as function of temperature is taken from Plummer and Busenberg (1982), and this expression yields $d\log_{10}(K_f(CaCO_3^0))/dT$ equal to 0.008715 at 25 °C.

The only quantity that the equilibrium constant $K_f(MgOH^+)$ contributes a significant uncertainty to is the ion product of water. The value of $K_f(MgOH^+)$ at 25 °C, based upon titration data for $MgCl_2$ solutions, is from the study of Harvie et al. (1984). They comment that a detailed reversible cell study of the $Mg(OH)_2$-$MgCl_2$-H_2O system would be useful in precisely characterizing the interactions of Mg^{2+}, OH^- and Cl^-. The variation with temperature of $K_f(MgOH^+)$ was estimated by Clegg and Whitfield (1991) from the data of Dickson and Riley (1979) for $K^*(H_2O)$ in seawater. This should be re-determined, from independent measurements.

The thermodynamic equilibrium solubility constant for calcite in the model is that of Plummer and Busenberg (1982), determined from measurements of solubility under fixed partial pressures of CO_2. Their treatment of speciation in the solutions involves both $CaHCO_3^+$ and $CaCO_3^0$ ion pairs. The equilibrium constant for the latter, 1675.3 kg mol^{-1} at 25 °C, is 18% greater than that in the present model, and the calculation of the activity coefficients differs. We found that the trend in the difference between measured and calculated $\ln(K^*(CaCO_{3(s)}))$ does not tend to zero as salinity decreases (Fig. 5b), which may indicate an incompatibility between the $K^*(CaCO_{3(s)})$ values of Plummer and Busenberg (1982) and the present model.

7.2. Activity coefficient parameters

Of the Pitzer parameters listed in Table 3, those for aqueous HCl, NaCl, $MgCl_2$, $CaCl_2$, and Na_2SO_4 are quite accurately known. For this group of pure (single solute) aqueous solutions, as well as for the mixture H^+-Na^+-Cl^--H_2O, there are multiple sets of available parameters, evaluated from a wide range of activity and thermal data. For this reason, we do not consider them likely to be significant contributors to errors in model predictions, compared to parameters for other combinations of ions.

Parameters for Na^+-HCO_3^- and Na^+-CO_3^{2-} interactions make large uncertainty contributions to the calculated $pH^*_{T,m}$ and the two carbonate equilibria. Both sets of parameters are from the study of Peiper and Pitzer (1982), and we identified in Section 6.1.1 that revisions to the Na^+-HCO_3^- parameters will probably yield improved predictions of $K^*(CO_2^*)$ across the salinity range. The two sets of parameters are not independent.

Deviations of calculated $\ln(K^*(CO_2^*))$ from the measurements are also temperature dependent (Fig. 2b), especially for high salinities (Fig. S1 of the eighth document of the Supporting Information). This behaviour could be associated with one or more interaction parameters, such as those for Na^+-HCO_3^-. Parameters $\theta_{Cl,HCO3}$ and $\psi_{Cl,HCO3,Na}$ also have a large influence on $K^*(CO_2^*)$, and their variation with temperature is unknown. However, Peiper and Pitzer (1982) found that only constant values were needed in order to fit their data. We note that, although the Mg^{2+}-HCO_3^- interaction parameters contribute only about 1% to the estimated total variance of the model calculated $\ln(K^*(CO_2^*))$ their variation with temperature is unknown (these parameters were determined from data at 25 °C only, by Pitzer et al. (1985)). Consequently, they could contribute significantly more to the total variance at other temperatures.

There are a number of inconsistencies in the sets of Pitzer parameters used for solutions containing $B(OH)_4^-$ that may explain features of the plots in Fig. 6 such as the fact that $\Delta\ln(K^*(B(OH)_4^-))$ do not tend to zero as salinity tends to zero. The Pitzer parameters for Na^+-$B(OH)_4^-$ interactions are those of Simonson et al. (1987) who also determined $\theta_{Cl,B(OH)4}$ (−0.056) and $\psi_{Na,B(OH)4,Cl}$ (−0.019). These mixture parameters do not vary with temperature. Simonson et al. (1988) determined Mg^{2+}-$B(OH)_4^-$ parameters but set $\psi_{Cl,B(OH)4,Mg}$ to zero. However, in the model $\theta_{Cl,B(OH)4}$ varies with T (and is −0.0323 at 25 °C), $\psi_{Cl,B(OH)4,Na}$ is −0.0132 and $\psi_{Cl,B(OH)4,Mg}$ is −0.235. This is an inconsistency. The sources of data used by Pierrot (2002) to determine $\theta_{Cl,B(OH)4}$ and $\psi_{Na,Cl,B(OH)4}$ in the model are the results of Hershey et al. (1986) and Owen and King (1945), and for $\psi_{Cl,B(OH)4,Mg}$ the results of Hershey et al. (1986) and Simonson et al. (1988) were used. Pierrot (2002) also included the formation of ion pair $MgB(OH)_4^+$ in his model. Simonson et al. (1988) discuss the differences between their results and those of Hershey et al. (1986), the significance of inconsistencies in the

thermodynamic treatments, and the differences between the compositions of the solutions on which measurements have been made and those typical in the environment (low borate and relatively high Mg^{2+}). The Pitzer parameters for borate interactions in solutions containing sodium and magnesium chloride solutions should be re-examined, together with the influence of polyborate formation on the properties of the solutions from which these parameters have been obtained.

Calculated saturation with respect to calcite, see Fig. 5b, is another example in which the deviations between measured and calculated ln (K^*) both have a salinity dependence, and do not tend to zero at zero salinity. At salinity 35, about half of the total dissolved CO_3^{2-} is predicted to be $MgCO_3^0$. The only interaction parameter for this species is that with Na^+ (relative to an interaction with Cl^- that is set to zero), for the temperature of 25 °C. Studies to determine interactions with SO_4^{2-} and those with Na^+ at different temperatures (in addition to the value of $K_f(MgCO_3^0)$ itself) would be valuable and result in a more accurate value of the $m{Mg^{2+}}\cdot K_f^*(MgCO_3^0)$ term in the expression for the total activity coefficient of CO_3^{2-} in Eq. (11).

The principal feature of the deviation plot for $\ln(K^*(H_2O))$ is the trend with salinity at 5 °C. Interactions of the ion pair $MgOH^+$ with Cl^- are only known only at 25 °C (and those with SO_4^{2-} are unknown). The only available ternary parameter is $\psi_{Mg,MgOH,Cl}$. Studies to determine the Pitzer parameters for $MgOH^+$-Cl^- and $MgOH^+$-SO_4^{2-} at different temperatures would be valuable.

Finally, we note that the thermodynamic equilibrium constants for many of the ion pairs, and for calcite, are determined from measurements of solution mixtures. The values derived from these measurements are dependent upon the treatment – generally a model – of the activity coefficients of the solute species involved, including any assumptions (such as being invariant with temperature, or set to zero). An examination of the calculation of these activity coefficients, to test their consistency with the present model and their influence on the derived equilibrium constants, is likely to be needed.

7.3. Other considerations

Here we summarise a number of general points to be considered when determining new or revised values of interaction parameters from measurements and data analysis.

- Suitable thermodynamic data for the determination of Pitzer interaction parameters are those that provide either directly, or indirectly, solute or solvent activities, or the thermal and volumetric properties that yield the temperature and pressure derivatives of the parameters (Pitzer, 1991). Experiments should be carried out on the simplest solutions (i.e., containing the fewest solute ions and/or neutral species) needed to determine the interaction parameters of interest. Thus, for example, parameters $\theta_{H,Na}$ and $\psi_{H,Na,Cl}$ can be determined from measurements of the activity product $a{H^+}\cdot a{Cl^-}$ in HCl-NaCl aqueous mixtures. This procedure cannot always be followed: a notable example is Na^+-HSO_4^- interactions for which the parameters are obtained from data for H_2SO_4-Na_2SO_4 solutions (e.g., Rard et al., 2000) in which the ions present are H^+, Na^+, HSO_4^-, and SO_4^{2-}. In such cases it is worthwhile considering the selection of solution compositions (e.g., the relative amounts of H_2SO_4 and Na_2SO_4) needed to best constrain the fitted parameters.
- For seawater applications the model needs to be most accurate below ionic strengths of about 1 mol kg^{-1}, but it is also true that Pitzer parameter values are determined most precisely from measurements in more highly concentrated solutions. Consequently, data over a wide range of molalities are desirable, but limited (at the upper end) so that model accuracy is not biased towards the representation of high ionic strength properties. Thermodynamic properties in general vary more steeply with temperature close to 0 °C than they do at higher temperatures (25 °C and above). Measurement at low temperatures, to determine values of interaction parameters close to 0 °C, are therefore desirable, as are measurements of thermal properties from which derivatives of interaction parameters with respect to temperature can be determined directly.
- Pitzer and Kim (1974) have shown how measured osmotic and activity coefficients can be used to determine $\theta_{ii'}$ and $\psi_{ii'j}$ as the intercept and slope, respectively, of linear fits with respect to a measure of total molality, and the application of the approach should be considered when designing experiments so as to obtain fitted $\theta_{ii'}$ and $\psi_{ii'j}$ with the smallest variances. It can also be worth examining the equations expressing the measured thermodynamic property in terms of species molalities and Pitzer model expressions for their activity coefficients in order to identify pairs or groups of parameters that cannot be determined independently from the measurements. Examples of this include the analysis of the results of titrations to obtain values of the acid dissociation constant of $TrisH^+$ ($K^*(TrisH^+)$) in salt solutions, and EMF measurements of cells containing dissolved $TrisH^+$ and Tris (e.g., see Eqs. (13) and (16) of Lodeiro et al., 2021). Values of the parameters $\theta_{TrisH,Na}$, $\theta_{H,Na}$, and $\lambda_{Tris,Na}$ can only be determined from the titration measurements as the quantity ($\theta_{TrisH,Na} - \theta_{H,Na} - \lambda_{Tris,Na}$). Of these three parameters, only $\theta_{H,Na}$ is known from other data. It is normal in such cases to set one of each pair of unknown parameters to zero (so that the other can be assigned a fitted value). It is important to explain these choices. The practical impact on model calculations depends upon the quantity of interest (there would be none, for example, on model simulations of $K^*(TrisH^+)$).
- The determination of model parameters for interactions of solute species that take part in reactions are a particular difficulty, because these require fitting data for solutions containing multiple components, sometimes only weakly constrained with respect to the molalities of individual ions and uncharged solutes. Examples include aqueous H_2SO_4 (containing H^+, HSO_4^- and SO_4^{2-}) (Clegg et al., 1994), and Na^+ - HCO_3^- - CO_3^{2-} - OH^- - Cl^- aqueous solutions (Peiper and Pitzer, 1982). Data for the H_2SO_4-Na_2SO_4 mixtures mentioned above are used to obtain Na^+-HSO_4^- interaction parameters, in combination with significant ternary parameters involving HSO_4^-, and Na^+ and/or SO_4^{2-}. In such cases experimental design – the composition of the solutions – can benefit from modelling to estimate the dominant species for particular solution compositions and therefore the parameters that have the greatest influence on the measured thermodynamic property.
- The development of models of the solution mixtures often involves choices as to what parameters are set to zero (because one or more may be poorly constrained by the data), and the relative weights given to different types of data. It is important that the rationale behind the choices is explained, and it is preferable that the parameters determined are fully consistent with others used in any larger model. We note, for example, that the Na^+-Cl^- and H^+-Cl^- interaction parameters in the treatment of Peiper and Pitzer (1982) are not the same as those adopted in the present model. The effects seem likely to be small, but should be examined in future.
- Variances, and covariances where possible, of fitted Pitzer parameters and/or equilibrium constants should be reported. Details of procedure (weights, rejected data) should also be presented, such that it is possible to reproduce the results.

8. Summary and discussion

In this work we have amended and documented the model of Millero and Pierrot (1998) and Pierrot and Millero (2017), and included the

Table 4
Summary of model-calculated pH, and approximate differences between measured and calculated equilibrium constants at salinity 35, and 25 °C.

Measure of pH [a]	Value ($S = 35$, at 25 °C)	σ (model) [b]	Equilibrium constant	~ΔpK* (meas. – model) [c]	σ (model) [d]
pH*$_{T,m}$	8.1023	0.014	K*(CO_2*)	+0.011	0.012
pH*$_{SW,m}$	8.0928	0.014	K*(HCO_3^-)	−0.011	0.018
pH*$_{F,m}$	8.2084	0.013	K*($B(OH)_4^-$)	+0.020	0.010

[a] Conventional thermodynamic pH on a molality basis, on the total (T), seawater (SWS) and free (F) scales, see Eqs. (1) and (2). The value of pH*$_{F,m}$ is equal to -$\log_{10}(mH^+)$.
[b] The estimated uncertainty of the model-calculated pH.
[c] This is the approximate difference ($S = 35$, and 25 °C) between accepted measured values of the pK* of the indicated equilibria, and the model-calculated value. These numbers were obtained from Figs. 2a, 3a and 6c.
[d] These are the estimated uncertainties in the model-calculated pK*.

propagation of uncertainties for the first time. We have assessed the performance of the model for acid-base speciation equilibria and identified, from the calculated uncertainty contributions and a review of source literature, those elements of the model that should be revised. In our comparisons of the model with available measurements of dissociation constants of the carbonate system in seawater it has become clear that for salinities below 10 improvements in the values of K*(HCO_3^-) are needed. For example, the p(K*(HCO_3^-)) from the dataset of Millero et al. (2006) are very scattered, and mostly appear to be too low.

The differences between model-calculated and measured equilibrium constants for the carbonate system and for borate are summarised in Table 4. The differences, in the ~ΔpK* column, are comparable in magnitude to the estimated uncertainties of the model-calculated values (last column), except for K*($B(OH)_4^-$) where the ~ΔpK* is a factor of two greater. Comparisons over a range of temperatures and salinities are shown in Figs. 2-4, 6, and Figs. S1–3 of the eighth document of the Supporting Information. Also listed in Table 4 are the calculated conventional thermodynamic pH for salinity 35 seawater at 25 °C. Of primary interest here are the differences between the scales: about −0.01 between pH*$_{SW,m}$ and pH*$_{T,m}$, and + 0.11 between pH*$_{F,m}$ and pH*$_{T,m}$. The difference between the total and seawater pH values is less than the scatter in the measured values of the carbonate constants at the same salinity and temperature, but not by a large margin.

The most appropriate use for the model, in its present state of development, is to estimate the effects of changes in the natural water medium from a seawater stoichiometry to some different composition. This can be done, for the value of a carbonate or borate stoichiometric dissociation constant for example, by first calculating the pK* value for the temperature of interest and the required salinity using one of the available empirical equations, and then a ΔpK* between that salinity and the composition of interest using the model. The two values are added together to obtain an estimated pK* for the natural water composition. For example, the model of Millero and Pierrot (1998), in its MYAMI version, has been used in this way by Hain et al. (2015) to investigate the effect of Mg^{2+} and Ca^{2+} concentration changes on seawater acid-base equilibria in past oceans. For this procedure to be most accurate the model needs to contain the Pitzer parameters that are relevant to that composition change. For example, it is desirable for a calculation of pK*(HCO_3^-) for a natural water with a different sulphate concentration than an equivalent seawater that the parameters for $MgCO_3^0$-SO_4^{2-} interactions are known (because $MgCO_3^0$ is calculated to account for about half of the total carbonate ion in seawater). If the model is used in this way it may be helpful to assess the likely sensitivity to the influence of the interaction parameters, especially those that remain unknown.

Future work should focus, first, on the improvements in the representation of the carbonate and borate equilibria in seawater, as outlined in the previous sections. The calculation of total pH, and conversion between total and free pH (i.e., H^+ amount content), are also important. The requirements for an improved model of solutions containing the ions of artificial seawater (particularly the HSO_4^-/SO_4^{2-} equilibrium), and the extension of model to include the Tris buffers used for calibration of total pH, have been described in papers (I) and (II). Unification of both models, so they contain the same equilibrium constants and Pitzer interaction parameters for the set of solute species in common, is also desirable.

Declaration of Competing Interest

None.

Data availability

No data were used for the research described in the article.

Acknowledgements

The work of S.L.C. was supported by the Natural Environment Research Council of the UK (award NE/P012361/1), and A.G.D. by the U.S. National Science Foundation (award OCE-1744653), both under the joint NERC/NSF:GEO scheme. The contribution of J.F.W. was supported by the National Institute of Standards and Technology of the U.S. A. This publication is a contribution of SCOR Working Group 145 (SCOR is the Scientific Committee on Oceanic Research) and of the Joint Committee on the Properties of Seawater which is sponsored by SCOR, the International Association for the Properties of Water and Steam, and the International Association for the Physical Sciences of the Oceans. The work of WG 145 presented in this article results, in part, from funding provided by national committees of SCOR and from a grant to SCOR from the U.S. National Science Foundation (OCE-1840868).

Appendix A. Supplementary data

There are nine documents of supporting information. The first document summarises the contents of the others, and lists the tables and charts that appear in each one. The subjects covered are: an overview of the model, and details of the simulation of uncertainties; values of variances and covariances for interactions and equilibrium constants for all species; values of the Pitzer parameters and equilibrium constants and their sources; and calculated equilibrium solute molalities and activity coefficients for program verification. It is anticipated that software tools incorporating the models will be released during 2023 (see website marchemspec.org for future announcements, or contact the corresponding author). The supplementary data to this article can be found online at https://doi.org/10.1016/j.marchem.2022.104196.

References

Archer, D.G., 1992. Thermodynamic properties of the NaCl + H_2O system II. Thermodynamic properties of NaCl(aq), NaCl.$2H_2O$(cr), and phase equilibria. J. Phys. Chem. Ref. Data 21, 793–829. https://doi.org/10.1063/1.555915.
Broene, H.H., De Vries, T., 1947. The thermodynamics of aqueous hydrofluoric acid solutions. J. Am. Chem. Soc. 69, 1644–1646. https://doi.org/10.1021/ja01199a022.
Clegg, S.L., Whitfield, M., 1991. Activity coefficients in natural waters. In: Pitzer, K.S. (Ed.), Activity Coefficients in Electrolyte Solutions, 2nd edn., CRC Press, Boca Raton, pp. 279–434.
Clegg, S.L., Whitfield, M., 1995. A chemical model of seawater including dissolved ammonia, and the stoichiometric dissociation constant of ammonia in estuarine water and seawater from −2 ° to 40 °C. Geochim. Cosmochim. Acta 59, 2403–2421. https://doi.org/10.1016/0016-7037(95)00135-2.
Clegg, S.L., Rard, J.A., Pitzer, K.S., 1994. Thermodynamic properties of 0-6 mol kg^{-1} aqueous sulphuric acid from 273.15 to 328.15 K. J. Chem. Soc. Faraday Trans. 90, 1875–1894. https://doi.org/10.1039/FT9949001875.
Clegg, S.L., Humphreys, M.P., Waters, J.F., Turner, D.R., Dickson, A.G., 2022. Chemical speciation models based upon the Pitzer activity coefficient equations, including the propagation of uncertainties. II. Tris buffers in artificial seawater at 25 °C, and an

assessment of the seawater 'Total' pH scale. Mar. Chem. 244 art. no. 104096, 24 pp. https://doi.org/10.1016/j.marchem.2022.104096.
DelValls, T.A., Dickson, A.G., 1998. The pH of buffers based on 2-amino-2-hydroxy-methyl-1,3-propanediol ("tris") in synthetic sea water. Deep-Sea Res. I 45, 1541–1554.
Dickson, A.G., 1990. Thermodynamics of the dissociation of boric acid in synthetic seawater from 273.15 to 318.15 K. Deep-Sea Res. 37, 755–766.
Dickson, A.G., Riley, J.P., 1979. The estimation of acid dissociation constants in seawater media from potentiometric titrations with strong base. I. The ionic product of water - K_w. Mar. Chem. 7, 89–99. https://doi.org/10.1016/0304-4203(79)90001-X.
Dickson, A.G., Sabine, C.L., Christian, J.R. (Eds.), 2007. Guide to Best Practices for Ocean CO_2 Measurements. North Pacific Marine Science Organisation. PICES Special Publication 3, IOCCP Report No. 8, 176 pp.
Dickson, A.G., Wesolowski, D.J., Palmer, D.A., Mesmer, R.E., 1990. Dissociation constant of bisulphate ion in aqueous sodium chloride solutions to 250 °C. J. Phys. Chem. 94, 7978–7985. https://doi.org/10.1021/j100383a042.
Doherty, L.A., Kester, D.R., 1974. Freezing point of sea water. J. Mar. Sci. 32, 285–300.
Douglas, N.K., Byrne, R.H., 2017. Spectrophotometric pH measurements from river to sea: calibration of mCP for $0 \leq S \leq 40$ and $278.15 \leq T \leq 308.15$ K. Mar. Chem. 197, 64–69. https://doi.org/10.1016/j.marchem.2017.10.001.
Elgquist, B., 1970. Determination of the stability constants of MgF^+ and CaF^+ using a fluoride selective electrode. J. Inorg. Nucl. Chem. 32, 937–944. https://doi.org/10.1016/0022-1902(70)80072-0.
Feistel, R., 2008. A Gibbs function for seawater thermodynamics for −6 to 80 °C and salinity up to 120 g kg^{-1}. Deep-Sea Res. I 55, 1639–1671.
Felmy, A.R., Weare, J.H., 1986. The prediction of borate mineral equilibria in natural waters - application to Searles Lake, California. Geochim. Cosmochim. Acta 50, 2771–2783. https://doi.org/10.1016/0016-7037(86)90226-7.
Fujino, K., Lewis, E.L., Perkin, R.G., 1974. The freezing point of seawater at pressures up to 100 bars. J. Geophys. Res. 79 (12), 1792–1797. https://doi.org/10.1029/JC079i012p01792.
Goyet, C., Poisson, A., 1989. New determination of carbonic acid dissociation constants in seawater as a function of temperature and salinity. Deep-Sea Res. 36 (11), 1635–1654.
Hain, M.P., Sigman, D.M., Higgins, J.A., Haug, G.H., 2015. The effects of secular calcium and magnesium concentration changes on the thermodynamics of seawater acid/base chemistry: implications for the Eocene and Cretaceous ocean carbon chemistry and buffering. Glob. Biogeochem. Cycles 29, 517–533. https://doi.org/10.1002/2014GB004986.
Hain, M.P., Sigman, D.M., Higgins, J.A., Haug, G.H., 2018. Response to comment by Zeebe and Tyrrell on "The effects of secular calcium and magnesium concentration changes on the thermodynamics of seawater acid/base chemistry: implications for the Eocene and Cretaceous ocean carbon chemistry and buffering". Glob. Biogeochem. Cycles 32, 898–901. https://doi.org/10.1002/2018GB005931.
Harned, H.S., Davis, R., 1943. The ionization constant of carbonic acid in water and the solubility of carbon dioxide in water and aqueous salt solutions from 0 to 50 °. J. Am. Chem. Soc. 65, 2030–2037. https://doi.org/10.1021/ja01250a059.
Harned, H.S., Owen, B.B., 1958. The Physical Chemistry of Electrolytic Solutions. Reinhold, New York.
Harned, H.S., Scholes, S.R., 1941. The ionization constant of HCO_3^- from 0 to 50 °. J. Am. Chem. Soc. 63, 1706–1709.
Harvie, C.E., Møller, N., Weare, J.H., 1984. The prediction of mineral solubilities in natural waters: the Na-K-Mg-Ca-H-Cl-SO_4-OH-HCO_3-CO_3-CO_2-H_2O system to high ionic strengths at 25 C. Geochim. Cosmochim. Acta 48, 723–751. https://doi.org/10.1016/0016-7037(84)90098-X.
He, S., Morse, J.W., 1993. The carbonic acid system and calcite solubility in aqueous Na-K-Ca-Mg-Cl-SO_4 solutions from 0 to 90 °C. Geochim. Cosmochim. Acta 57, 3533–3554. https://doi.org/10.1016/0016-7037(93)90137-L.
Hershey, J.P., Fernandez, M., Milne, P.J., Millero, F.J., 1986. The ionization of boric acid in NaCl, Na-Ca-Cl and Na-Mg-Cl solutions at 25 C. Geochim. Cosmochim. Acta 50, 143–148. https://doi.org/10.1016/0016-7037(86)90059-1.
Humphreys, M.P., Waters, J.F., Turner, D.R., Dickson, A.G., Clegg, S.L., 2022. Chemical speciation models based upon the Pitzer activity coefficient equations, including the propagation of uncertainties: artificial seawater from 0 to 45 °C. Mar. Chem. 244 art. no. 104095, 23 pp. https://doi.org/10.1016/j.marchem.2022.104095.
Klotz, I.M., Rosenberg, R.M., 1972. Chemical Thermodynamics, Basic Theory and Methods, 3rd ed., Benjamin/Cummings, Menlo Park.
Lewis, E.L., Wallace, D., 1998. Program Developed for CO_2 System Calculations. ORNL/CDIAC-105. Carbon Dioxide Information Analysis Centre, Oak Ridge National Laboratory.
Liu, X., Patsavas, M.C., Byrne, R.H., 2011. Purification and characterization of meta-cresol purple for spectrophotometric seawater pH measurements. Environ. Sci. Technol. 45, 4862–4868. https://doi.org/10.1021/es200665d.
Lodeiro, P., Turner, D.R., Achterberg, E.P., Gregson, F.K.A., Reid, J.P., Clegg, S.L., 2021. Solid – liquid equilibria in aqueous solutions of Tris, Tris-NaCl, Tris-TrisHCl, and Tris-$(TrisH)_2SO_4$ at temperatures from 5 °C to 45 °C. J. Chem. Eng. Data 66, 437–455.
Lueker, T.J., Dickson, A.G., Keeling, C.D., 2000. Ocean pCO_2 calculated from dissolved inorganic carbon, alkalinity, and equations for K_1 and K_2: validation based on laboratory measurements of CO_2 in gas and seawater at equilibrium. Mar. Chem. 70, 105–119. https://doi.org/10.1016/S0304-4203(00)00022-0.
Marshall, W.L., Franck, E.U., 1981. Ion product of water substance, 0 °C-1000 °C, 1-10,000 bars - new international formulation and its background. J. Phys. Chem. Ref. Data 10, 295–304. https://doi.org/10.1063/1.555643.
Millero, F.J., 2010. Carbonate constants for estuarine waters. Mar. Freshw. Res. 61, 139–142. https://doi.org/10.1071/MF09254.
Millero, F.J., Pierrot, D., 1998. A chemical equilibrium model for natural waters. Aquat. Geochem. 4, 153–199. https://doi.org/10.1023/A:1009656023546.
Millero, F.J., Roy, R.N., 1997. A chemical equilibrium model for the carbonate system in natural waters. Croat. Chem. Acta 70, 1–38.
Millero, F.J., Thurmond, V., 1983. The ionization of carbonic acid in Na-Mg-Cl solutions at 25 °C. J. Solut. Chem. 12, 401–411.
Millero, F.J., Graham, T.B., Huang, F., Bustos-Serrano, H., Pierrot, D., 2006. Dissociation constants of carbonic acid in seawater as a function of salinity and temperature. Mar. Chem. 100, 80–94. https://doi.org/10.1016/j.marchem.2005.12.001.
Millero, F.J., Feistel, R., Wright, D.G., McDougall, T.J., 2008. The composition of standard seawater and the definition of the reference-composition salinity scale. Deep-Sea Res. I 55, 50–72.
Møller, N., 1988. The prediction of mineral solubilities in natural waters: a chemical equilibrium model for the Na-Ca-Cl-SO_4-H_2O system, to high temperature and concentration. Geochim. Cosmochim. Acta 52, 821–837. https://doi.org/10.1016/0016-7037(88)90354-7.
Mucci, A., 1983. The solubility of calcite and aragonite in seawater at various salinities, temperatures and one atmosphere pressure. Am. J. Sci. 283, 780–799. https://doi.org/10.2475/ajs.283.7.780.
Nordstrom, D.K., Plummer, N.L., Langmuir, D., 1990. Revised chemical equilibrium data for major water mineral reactions and their limitations. In: Melchior, D.C., Bassett, R.L. (Eds.), Chemical Modelling in Aqueous Systems II. American Chemical Society, Washington, D.C., pp. 398–413
Orr, J.C., Epitalon, J.-M., Dickson, A.G., Gattuso, J.-P., 2018. Routine uncertainty propagation for the marine carbon dioxide system. Mar. Chem. 207, 84–107. https://doi.org/10.1016/j.marchem.2018.10.006.
Owen, B.B., 1934. The dissociation constant of boric acid from 10 to 50°. J. Am. Chem. Soc. 56, 1695–1697. https://doi.org/10.1021/ja01323a014.
Owen, B.B., King, E.J., 1945. The effect of sodium chloride upon the ionization of boric acid at various temperatures. J. Am. Chem. Soc. 65, 1612–1620.
Peiper, J.C., Pitzer, K.S., 1982. Thermodynamics of aqueous carbonate solutions including mixtures of sodium carbonate, bicarbonate and chloride. J. Chem. Thermodyn. 14, 613–638. https://doi.org/10.1016/0021-9614(82)90078-7.
Pierrot, D., 2002. Thermodynamic Investigations Using the Pitzer Formalism: Extension of the Model and its Applications. Ph.D. thesis, University of Miami, Miami, FL, 288 pp.
Pierrot, D., Millero, F.J., 2017. The speciation of metals in natural waters. Aquat. Geochem. 23 (1), 1–20. https://doi.org/10.1007/s10498-016-9292-4.
Pierrot, D., Millero, F.J., Roy, L.N., Roy, R.N., Doneski, A., Niederschmidt, J., 1997. The activity coefficients of HCl in HCl-Na_2SO_4 solutions from 0 to 50 °C and ionic strengths up to 6 molal. J. Solut. Chem. 26, 31–45. https://doi.org/10.1007/BF02439442.
Pitzer, K.S., 1991. Ion interaction approach: Theory and data correlation. In: Pitzer, K.S. (Ed.), Activity Coefficients in Electrolyte Solutions, 2nd edn., CRC Press, Boca Raton, pp. 75–153.
Pitzer, K.S., Kim, J., 1974. Thermodynamics of electrolytes IV: activity and osmotic coefficients of mixed electrolytes. J. Am. Chem. Soc. 96, 5701–5707. https://doi.org/10.1021/ja00825a004.
Plummer, L.N., Busenberg, E., 1982. The solubilities of calcite, aragonite and witerite in CO_2-H_2O solutions between 0 and 90 °C, and an evaluation of the aqueous model for the system $CaCO_3$-CO_2-H_2O. Geochim. Cosmochim. Acta 46, 1011–1040. https://doi.org/10.1016/0016-7037(82)90056-4.
Plummer, L.N., Parkhurst, D.L., Fleming, G.W., Dunkle, S.A., 1988. A Computer Program Incorporating Pitzer's Equations for Calculation of Geochemical Reactions in Brines. Water-Resources Investigations Report 88-4153. U.S. Geological Survey, Reston, VA.
Prieto, F.J.M., Millero, F.J., 2002. The values of $pK_1 + pK_2$ for the dissociation of carbonic acid in seawater. Geochim. Cosmochim. Acta 66, 2529–2540. (This publication is indexed using the author name 'Prieto', rather than 'Mojica Prieto'.) https://doi.org/10.1016/S0016-7037(02)00855-4.
Rard, J.A., Platford, R.F., 1991. Experimental methods: Isopiestic. In: Pitzer, K.S. (Ed.), Activity Coefficients in Electrolyte Solutions, 2nd edn., CRC Press, Boca Raton, pp. 209–277.
Rard, J.A., Palmer, D.A., Clegg, S.L., 2000. Isopiestic Determination of the Osmotic Coefficients of Na_2SO_4(Aq) at 25 and 50 Degrees C, and Representation with Ion-Interaction (Pitzer) and Mole Fraction Thermodynamic Models.
Robinson, R.A., 1954. The vapour pressure and osmotic equivalence of sea water. J. Mar. Biol. Assoc. UK 33, 449–455.
Roy, R.N., Roy, L.N., Vogel, K.M., Porter-Moore, C., Pearson, T., Good, C.E., Millero, F.J., Campbell, D.M., 1993a. Thermodynamics of the dissociation of boric acid in seawater at S = 35 from 0 to 55 °C. Mar. Chem. 44, 243–248.
Roy, R.N., Roy, L.N., Vogel, K.M., Porter-Moore, C., Pearson, T., Good, C.E., Millero, F.J., Campbell, D.M., 1993b. The dissociation constants of carbonic acid in seawater at salinities 5 to 45 and temperatures 0 to 45 °C. Mar. Chem. 44, 249–267.
Roy, R.N., Roy, L.N., Vogel, K.M., Porter-Moore, C., Pearson, T., Good, C.E., Millero, F.J., Campbell, D.M., 1994. Erratum: the dissociation constants of carbonic acid in seawater at salinities 5 to 45 and temperatures 0 to 45 °C, Mar. Chem. 44, 249-267. Mar. Chem. 45, 337.
Roy, R.N., Roy, L.N., Vogel, K.M., Porter-Moore, C., Pearson, T., Good, C.E., Millero, F.J., Campbell, D.M., 1996. Erratum: the dissociation constants of carbonic acid in seawater at salinities 5 to 45 and temperatures 0 to 45 °C, Mar. Chem. 44: 249-267. Mar. Chem. 52, 183. https://doi.org/10.1016/0304-4203(96)83094-5.
Schockman, K.M., Byrne, R.H., 2021. Spectrophotometric determination of the bicarbonate dissociation constant in seawater. Geochim. Cosmochim. Acta 300, 231–245. https://doi.org/10.1016/j.gca.2021.02.008.

Simonson, J.M., Roy, R.N., Roy, L.N., Johnson, D.A., 1987. The thermodynamics of aqueous borate solutions I. Mixtures of boric acid with sodium or potassium borate and chloride. J. Solut. Chem. 16, 791–803.

Simonson, J.M., Roy, R.N., Mrad, D., Lord, P., Roy, L.N., Johnson, D.A., 1988. The thermodynamics of aqueous borate solutions. II. Mixtures of boric acid with calcium or magnesium borate and chloride. J. Solut. Chem. 17, 435–446.

Soli, A.L., Byrne, R.H., 2002. CO_2 system hydration and dehydration kinetics and the equilibrium CO_2/H_2CO_3 ratio in aqueous NaCl solution. Mar. Chem. 78, 65–73. https://doi.org/10.1016/S0304-4203(02)00010-5.

Turner, D.R., Achterberg, E.P., Chen, C.-T.A., Clegg, S.L., Hatje, V., Maldonado, M.T., Sander, S.G., van den Berg, C.M.G., Wells, M., 2016. Toward a quality-controlled and accessible Pitzer model for seawater and related systems. Front. Mar. Sci. 3, art. 139. https://doi.org/10.3389/fmars.2016.00139.

Waters, J.F., Millero, F.J., 2013. The free proton concentration scale for seawater pH. Mar. Chem. 149, 8–22. https://doi.org/10.1016/j.marchem.2012.11.003.

Waters, J.F., Millero, F.J., Woosley, R.J., 2014. Corrigendum to "The free proton concentration scale for seawater pH", [MARCHE: 149 (2013) 8–22]. Mar. Chem. 165, 66–67. https://doi.org/10.1016/j.marchem.2014.07.004.

Wexler, A.S., Clegg, S.L., 2002. Atmospheric aerosol models for systems including the ions H^+, NH_4^+, Na^+, SO_4^{2-}, NO_3^-, Cl^-, Br^-, and H_2O. J. Geophys. Res. 107, art. no. 4207.